ECMWF RE-ANALYSIS

ERA-40 Project Report Series

6. Evaluation of the ERA-40 surface water budget and surface temperature for the Mackenzie River basin

Alan K. Betts[1], John H. Ball[1] and Pedro Viterbo

[1] Atmospheric Research, Pittsford, VT

European Centre for Medium-Range Weather Forecasts
Europäisches Zentrum für mittelfristige Wettervorhersage
Centre européen pour les prévisions météorologiques à moyen terme

ECMWF RE-ANALYSIS ERA

ERA-40 Project Report Series

6. Evaluation of the ERA-40 surface water budget and surface temperature for the Mackenzie River basin

Alan K. Betts[1], John H. Ball[1] and Pedro Viterbo

[1] Atmospheric Research, Pittsford, VT

European Centre for Medium-Range Weather Forecasts
Europäisches Zentrum für mittelfristige Wettervorhersage
Centre européen pour les prévisions météorologiques à moyen terme

Evaluation of the ERA-40 surface water budget and surface temperature for the Mackenzie River basin

Alan K. Betts[1], John H. Ball[1] and Pedro Viterbo

Research Department

[1] Atmospheric Research, Pittsford, VT

For additional copies please contact

The Library
ECMWF
Shinfield Park
Reading, Berks RG2 9AX

library@ecmwf.int

Series: ECMWF ERA40 Project Report Series

A full list of ECMWF Publications can be found on our web site under:
http://www.ecmwf.int/publications/

Abstract

We assess the systematic biases in temperature and precipitation, and the surface water budget of ERA-40 for the Mackenzie River basin by comparing monthly averages from ERA-40 with basin averages of surface observations of temperature, precipitation, evaporation and streamflow from the Mackenzie GEWEX (Global Energy and Water Cycle Experiment) Study (MAGS). The bias and spinup of precipitation in ERA-40 changes significantly over the analysis period, because of changes in the assimilated data. On an annual basis, both precipitation bias and spinup are correlated with the analysis increment of atmospheric total column water vapor. ERA-40 has in addition a high bias of precipitation in Spring and a low bias in Fall. The monthly precipitation analysis is best for the most recent decade, when the bias of the 0-12h forecast precipitation is only a few percent higher than the MAGS observations. Annual evapotranspiration from ERA-40 is higher than a MAGS estimate by 30%. The annual runoff in ERA-40 is comparable to the annual streamflow, but the interannual variability is poorly correlated. ERA-40 has two runoff peaks: in April, when snowmelt runs off quickly over the frozen ground, and in August, when the lowest model layer melts and reaches a soil moisture threshold, when deep drainage increases rapidly. In the model liquid water budget, the soil water analysis increment contributes only 17mm of water to the annual liquid budget (primarily in summer), small compared with the mean rainfall (323mm) and snowmelt (194mm). However in the frozen budget, the analysis increment of snow water equivalent, with an annual mean total of 97mm, is not much smaller than the mean annual snowfall (140mm). This is clearly an undesirable feature, which impacts the liquid budget through the snowmelt. Improvements to the model snow treatment are needed: snow melts too soon in the model, and is replaced by the snow analysis increments. For the Mackenzie, ERA-40 has a distinct seasonal temperature bias, with a 2 to 3K warm bias from December to April, and a cool bias in summer, reaching -1.5K in July. This signal is larger for the heavily forested southern basins. The warm winter bias may be related to a too-low albedo for snow under tall vegetation, which was greatly reduced to correct a much larger cold bias in an earlier version of the land-surface model (Viterbo and Betts, 1999). The cool summer bias may indicate excess evaporation. In a comparison of the sub-basins with the MAGS estimates, ERA-40 has more precipitation than the MAGS observations for the northern and western mountainous basins, but for those basins the data are sparse. For evaporation, ERA-40 has less variation across the basins than the MAGS estimate. ERA-40 appears to represent well the climatological gradient of deep soil temperature across the Mackenzie basin, from continuous permafrost in the north to no permafrost in the south.

1. Introduction

An important objective of the Global Energy and Water Cycle Experiment (GEWEX) is to improve our ability to simulate both water and energy exchange processes in global climate and weather models. The Mackenzie GEWEX Study (MAGS: Stewart et al., 1998; Stewart, 2002; Rouse et al., 2003) was designed to address some of the high latitude issues, where snow and ice play an important role in the surface energy exchanges. In an earlier paper (Betts and Viterbo, 2000), we discussed the hydrological budgets and surface energy balance for sub-basins of the Mackenzie River, using data from two years of the operational model of the European Centre for Medium-range Weather Forecasts (ECMWF). This paper continues this work, with data from the ECMWF 40-year reanalysis (ERA-40), which actually covers the 44 years, 1968-2001. ERA-40 was run in several parallel streams (Simmons and Gibson, 2000). The analysis system uses a recent version of the model physics, including the land-surface scheme described in Van den Hurk et al. (2000), and a 3-D variational assimilation system. The horizontal resolution of the spectral model is triangular truncation at T_L-159, and there are 60 levels in the vertical, including a well-resolved boundary layer and stratosphere. Documentation of the Integrated Forecast System (IFS), cycle 23r4, and a summary and discussion of the observations available at different times during the 40-year reanalysis can be found at http://www.ecmwf.int/research/era/ . Surface energy and water budgets, and near-surface and sub-surface variables averaged over river basins, are computed and archived during the analysis cycle at an hourly timescale. In this paper, using monthly means and datasets derived from MAGS

observations, we assess the systematic biases in temperature and the surface energy and water budgets of ERA-40. Another paper addresses these biases for the Mississippi basin (Betts et al., 2003). Walsh et al. (1998) compared observational estimates of Arctic precipitation and evaporation with 24 climate model simulations, and found these climate models overestimated high latitude precipitation.

MAGS has yielded several important observational studies. Stewart et al. (2000), Rouse (2000a), and Rouse et al. (2003) discuss the broad seasonal and regional character of the energy and water budgets of the Mackenzie, observational studies of the snow and lake hydrology, and developments in modeling. More detailed analyses of shallow lakes and northern wetlands, underlain by ice-rich permafrost, are presented in Rouse (2000b). The difficulty of closing the atmospheric moisture budget using rawinsonde data, and reconciling it with the surface water budget, is outlined in Strong et al. (2002). In the same special issue on MAGS, several papers (Louie et al. 2002; Cao et al. 2002) analyze in detail the unusual 1994-1995 water year, in which the 1995 spring melt was the earliest on record (Marsh et al. 2002).

2. River Basin Intercomparisons

For ERA-40, averages over selected basins are output for hourly time intervals (accumulated from the full time resolution data) for selected river basins. We averaged the hourly data up to one month, as discussed below. The representation of the Mackenzie River basins in ERA-40 is shown in Figure 1. The ERA-40 averages are over all gridpoints, indicated as green dots, inside each red polygon, which are approximations to the actual river basin boundaries shown in brown. Basin 1 is the Peel basin (and it includes the Mackenzie delta); 2 is the Great Bear Lake basin; 3 is Great Slave Lake; 4 is the Liard basin; basin 5 is the Peace River, which is represented by 2 quadrilaterals, 5A and 5B (with 5A being a rather poor fit to the eastern part); and basin 6 is the Athabasca River. All our results will be presented as these area averages. Table 1 lists the basin drainage areas, their approximation in the ECMWF model and their mean elevation, as well as the standard deviation (SD), maximum and minimum heights, all calculated on the model grid.

Table 1. Mackenzie sub-basin drainage areas and their model representation

|	Sub-Basin	Drainage Area (km^2)	ERA40 Area	Model Elevation			
	(km^2)			Mean	SD	max	min
						(m)	
1	Peel	117127	108187	686	384	1284	121
2	Great Bear Lake	421191	367573	478	361	1506	187
3	Great Slave Lake	378245	418757	348	99	565	196
4	Liard	273395	283920	991	315	1515	412
5	Peace	319110	344659				
	5A (E)		(206549)	573	198	1122	286
	5B (W)		(138110)	1147	213	1482	782
6	Athabasca	285111	260982	651	333	1611	358
	TOTAL	1791857	1784078				
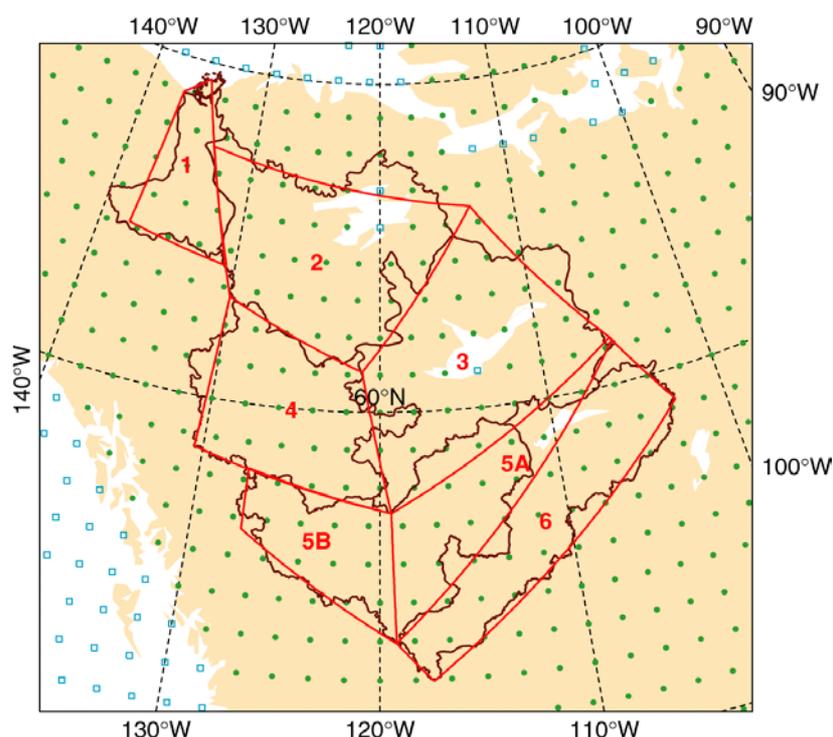
Figure 1River basin budgets in ERA-40 for the Mackenzie

2.1 Monthly averages from short-term forecasts

The model analysis cycle uses 6-hour forecasts from analyses at 00, 06, 12, and 18 UTC. From the 00 and 12 UTC analyses, forecasts were extended to 36 hours. Three monthly averages were constructed from twice-daily segments of the 0-12, 12-24, 24-36 hour forecasts, verifying at the same time. They will be identified by the notation 0-12h FX, etc. We shall use these to look at the spinup of the model fields and fluxes (specifically precipitation) in the first 36 hours. We also constructed monthly averages from the four 6-hourly segments of the analysis cycle, which we shall use to discuss the closure of the water budget in the model, which includes the modification of soil moisture and snow depth in the analysis cycle. For a few years (1958, 1973, 1989-1994), which were at the beginning of the ERA-40 analysis streams, basin averages of the 06 and 18 UTC 6-hour forecasts were not archived, so these years are excluded from the analysis of water budget closure. Fortunately, combining the two 0-12 hour forecasts from 00 and 12 UTC gives almost the same daily precipitation fluxes as combining the four 0-6 hour forecasts.

2.2 Distribution of vegetation in ERA-40

The land-surface scheme in ERA-40 has separate tiles for high (that is forests) and low vegetation classes, that are treated differently (Van den Hurk et al., 2000). At high latitudes the primary difference is that there is a tile for "high vegetation with snow beneath", which has a distinct energy budget for the snow layer, that is only partly coupled to the boundary layer. In addition, snow beneath forests has a much lower albedo (15%) to represent the shading effect of the canopy, than snow lying on top of low vegetation (whether tundra, marsh or cropland). The model does not represent snow on the tree canopy, nor does it have a model for the horizontal redistribution of snow on the sub-grid scale. Earlier land-surface schemes in the ECMWF model had too high an albedo for the boreal forests in winter (Viterbo and Betts, 1999), and after this was corrected too much evaporation of snow in winter (Betts et al. 1998, 2001b).

In ERA-40, each grid square now has a fraction and type of both high and low vegetation. The distribution across the Mackenzie basin of these is shown in Table 2. There is a transition from low vegetation (primarily tundra) being dominant in the north to more than 90% forest in the south. Basins 2 and 3 (Great Bear and Great Slave) have a small percent of water, in fact each has a single "lake point" at the T-159 resolution of ERA-40, but the impact of these on our analysis is small.

Table 2. Distribution of vegetation across the Mackenzie in ERA-40 as % of basin.

Basin	1	2	3	4	5A	5B	6
HIGH VEG.	**44**	**56**	**64**	**77**	**90**	**92**	**91**
evergreen needleleaf [3]			26	13	25	49	69
deciduous broadleaf [5]	43	17	32	51	55	43	
interrupted forest [19]	1	39	5	12	10		21
LOW VEG.	**56**	**40**	**33**	**23**	**10**	**7**	**9**
Tundra [9]	53	15	10	23		5	1
bogs/marsh [13]	3	25	6		2		1
deciduous shrubs [17]			17		1		4
crops/mixed farming [1]					7	2	3
Water		4	3				

2.3   Available surface observations

The observations available to validate the model are limited, since data is sparse in the Mackenzie basin. MAGS has produced three basin-averaged monthly products. Precipitation and temperature from 1950-1997 were produced by Louie et al. (2002). Climate station density is quite sparse in the Mackenzie basin, as shown in Figure 2. Of the 194 stations shown (with records >25 years), only 46 lie within or on the Mackenzie River basin boundary. There are more stations in the south in the Athabasca and Peace basins, a few in the Liard, and around
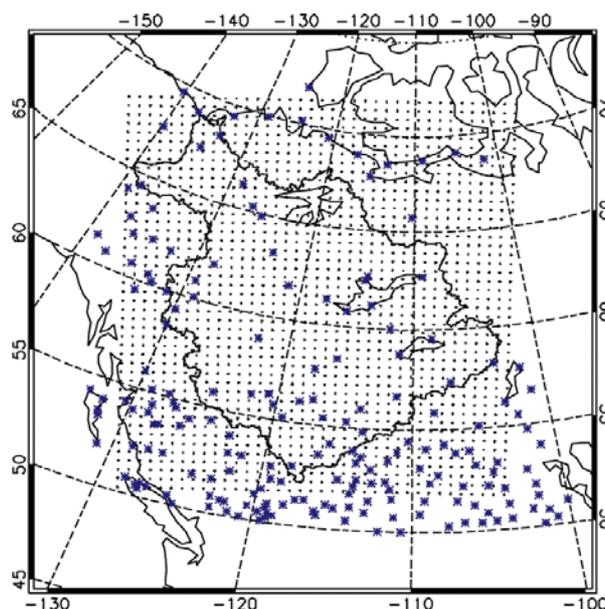

Figure 2 Long term (>25 years record)climate stations in or near the Mackenzie basin (from Louie et al. 2002)

Great Slave Lake, but only one within the Peel basin, and a few on the perimeter. Monthly mean fields cannot be generated directly from station data. Precipitation data were first corrected for all known measurement errors (Louie et al., 1996; Mekis and Hogg, 1999; Metcalfe et al., 1997). A first-guess field of 30-year normal temperature and precipitation (Seglenieks and Soulis, 2000) was constructed on the 0.5 degree grid shown in Figure 2. Monthly deviations of station data from the station normals were optimally interpolated to this grid (for precipitation, the deviations were first further normalized by the normal precipitation). Monthly mean maps of temperature and precipitation were then produced (Louie et al., 2002) by combining the normal and departures grids, and these were averaged over the six Mackenzie sub-basin drainages in Table 1, and the Mackenzie as a whole.

An estimate of evaporation from 1953-1996 was produced on the same grid by Louie et al. (2002), based on the method of Morton (1983). Morton's model is a semi-empirical method, which uses the air temperature, the dew-point, the percentage of possible sunshine, the latitude, the elevation, and the precipitation. Monthly averages were produced for the Mackenzie and the sub-basins.

We also have monthly stream flow data (HYDAT, 2000), with a range of record lengths, some back to 1958, which we have used to estimate the annual stream flow for most of our sub-basins, and the monthly stream flow for the Mackenzie as a whole. For comparison with model runoff, we converted all stream flow estimates to mm by dividing by the area drained by a given gauge. Table 3 lists the gauges with their location and drainage area, and which basin comparisons they were used for.

Table 3. Stream flow gauges used for basin estimations.

Gauge	Location	Drainage km^2	Basin estimation
10LC014 Mackenzie River at Arctic Red River [1972-2000]	67 27 30 N 133 44 41W	1,680,000	Mackenzie, Sum of 2,3,4,5,6,7
10MC002 Peel River above Fort McPherson	67 14 56 N 134 52 59 W	70,600	Mackenzie and 1
10LA002 Arctic Red River near the Mouth	66 47 24 N 133 04 54 W	18,600	Mackenzie and 1
10GC001 Mackenzie River at Fort Simpson	61 52 07 N 121 21 25 W	1,270,000	Sum of 3,4,5,6,7
10ED002 Liard River near the mouth [1972-2000]	61 44 34 N 121 13 40 W	2,275,000	4
07KC001 Peace River at Peace Point [1959-2000]	59 06 50 N 112 25 35 W	293,000	Sum of 5A, 5B
07HA001 Peace River at Peace River [1959-2000]	56 14 41 N 117 18 46 W	186,000	5B
07DA001 Athabasca River below McMurray	56 46 50 N 111 24 00 W	133,000	6

We estimated the monthly stream flow (converted to mm month^{-1}) for the Mackenzie River near its mouth by summing the first three in Table 3. For all the sub-basins (except 3: Great Slave Lake), we made estimates of the stream flow and stream flow difference (converted to mm by dividing stream flow by drainage area) using selected gauges as indicated in Table 3. Basin 1 was estimated by summing the Peel River and Arctic Red River (which does not include the Mackenzie delta). For basin 2, we subtracted the Mackenzie River flow at Fort Simpson from that at the Arctic Red River (note however that we have no estimates of the large storage within

the basin). For basin 3 we have no estimate, primarily because of missing data at the Mackenzie gauge near Fort Providence (not shown). The Liard River gauge near the mouth is representative of basin 4. The Peace River at Peace Point gives us the sum for our basins 5A and 5B. We made an estimate for the western half of the Peace basin, 5B, from the gauge at Peace River. An estimate for our eastern basin 5A was then found by difference. The flow on the western branch of the Peace after 1970 is heavily regulated by the completion of the Bennett dam in the late 1960's (see later). The last gauge was used as representative of the Athabasca basin 6, although note that it has a smaller drainage area than the model basin, and represents only the western part of the basin. Since we have no estimates of basin storage, comparisons of streamflow with runoff from ERA-40, which has no routing model, can provide only limited information on the water budget, primarily at annual timescales.

3. 44-year Overview

The idea of renanalysis is to use one recent 'frozen' model and data assimilation system to cover the entire period, in contrast to operational analyses in which the modeling system is revised on a frequent basis, as improved numerical or data assimilation schemes and physical parameterizations are introduced, along with increases in resolution. However, although the model is frozen, the data going into the reanalysis has changed markedly in the 44 years from 1958 to 2001, and this has a major impact on the analyses. There are three important epochs in ERA-40: 1958-1972, before "satellite data", when the upper air analysis depends on the sounding data; 1973-1986, starting with the assimilation of the radiances from the first satellite infrared channels on the Vertical Temperature Profiler Radiometer (VTPR) and, from late 1978, infrared and microwave sounders from the Television and Infrared Observational Satellite Operational Vertical Sounder (TOVS) suite of instruments; 1987-2001, with the addition of information of radiances from the satellite microwave channels of the Special Sensor Microwave Imager (SSM/I) to the atmospheric water vapor assimilation over the ocean.

As satellites are replaced, they are compared during their overlap period, and bias corrections are introduced for each satellite. However, these corrections do not remove all the inhomogeneities in the record. In addition, aerosols from volcanic eruptions, such as Pinatubo in 1991/2, affect the infrared emission, and have not been properly accounted for in ERA-40 (Kållberg, 2002, personal communication). There are also many changes in the conventional data, and over the Mackenzie in particular there is less data in the 1960's. In the next section, we show how the spinup of the model precipitation has changed markedly with time, and how it depends on the atmospheric moisture analysis. In general, the fit to precipitation observations has improved with time.

3.1 Model Precipitation spin-up and bias

3.1.1   *Change of spinup and bias with time*

The model hydrological cycle is not in balance during the 6-hour analysis cycle. Precipitation generally increases in ERA-40 in mid- and high latitudes during the first 36 hours of forecasts. This spin-up of precipitation varies considerably over the period of the reanalysis. The upper panel in Figure 3 shows, on the left hand scale, the annual precipitation from the MAGS data and the annual ERA-40 precipitation from the 0-12h forecasts (FX). On the right is the column soil moisture (CSM) in the model. We see that the model has a low bias of precipitation compared to the observations in the early 1960s, and CSM is correspondingly low; while in the middle 1970s, the model has a high bias in precipitation and correspondingly the highest mean soil moisture. The lower panel plots on the left hand scale, the spinup of model precipitation from the 0-12h to the 24-36h FX, and its components: convective precipitation (CP), and large-scale precipitation (LSP), which is the dominant

term. The right hand-scale shows the bias of the 0-12h FX precipitation from the MAGS observations (the scale is both different and inverted). The trend of the bias mirrors quite closely the model spinup on a annual basis from large negative bias at the beginning of ERA-40, coupled with a large spinup, to a positive bias in the middle 1970's with the smallest spinup, to finally the smallest bias in the 1990s with an intermediate spinup of precipitation.
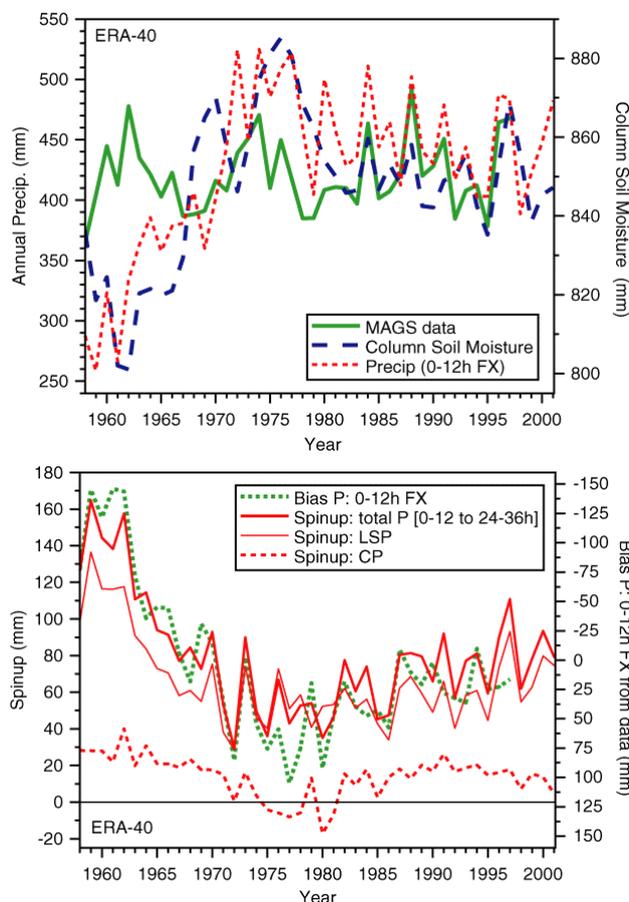

Figure 3 Annual mean precipitation in model and MAGS observations and column soil moisture (top); model precipitation spinp and bias from observations (bottom).

This change of bias and spinup with time appears to be linked to changes in the analysis increment of water vapor during the 44 years. Figure 4 (upper panel) shows the annual mean atmospheric total column water vapor (TCWV) and the analysis increment of TCWV. The increment, on the right-hand-scale, shows a drift with time from a negative value at the start of the reanalysis to near zero or positive in the mid-1970s to again negative in the 1990s. The TCWV in the analysis has a significant upward drift in the 1960s, which we believe is spurious. The middle and lower panels show that both the bias of the model 0-12h FX precipitation from the MAGS observations, and the spinup of model precipitation are correlated with the TCWV analysis increment. The analysis removes TCWV, which reduces precipitation in the analysis cycle, and the model then spins up to restore precipitation. For the period 1974-1981, when the analysis increment is near zero, the spinup is a minimum. For the same period, the mean bias is +66mm, 16% of the MAGS precipitation, and within the probable error of the observations. Since precipitation is the primary driver of the hydrological cycle, this spinup variation over the 44 years of ERA-40 is of fundamental importance, and it is being investigated further. Initially we thought that the different epochs of satellite data were the primary driver. However the large ramp of spinup,

bias and TCWV analysis increment seen in the 1960s appears complete by 1972, just before the incorporation of the VTPR satellite data, so changes in the conventional data (or its use) must be responsible for this shift. One source of error has been identified. The atmospheric humidity in one of the datasets used for the period 1958-1963 had a dry bias, up to several g kg-1 in summer, due to an unit conversion problem. This had the largest impact over the North American continent.
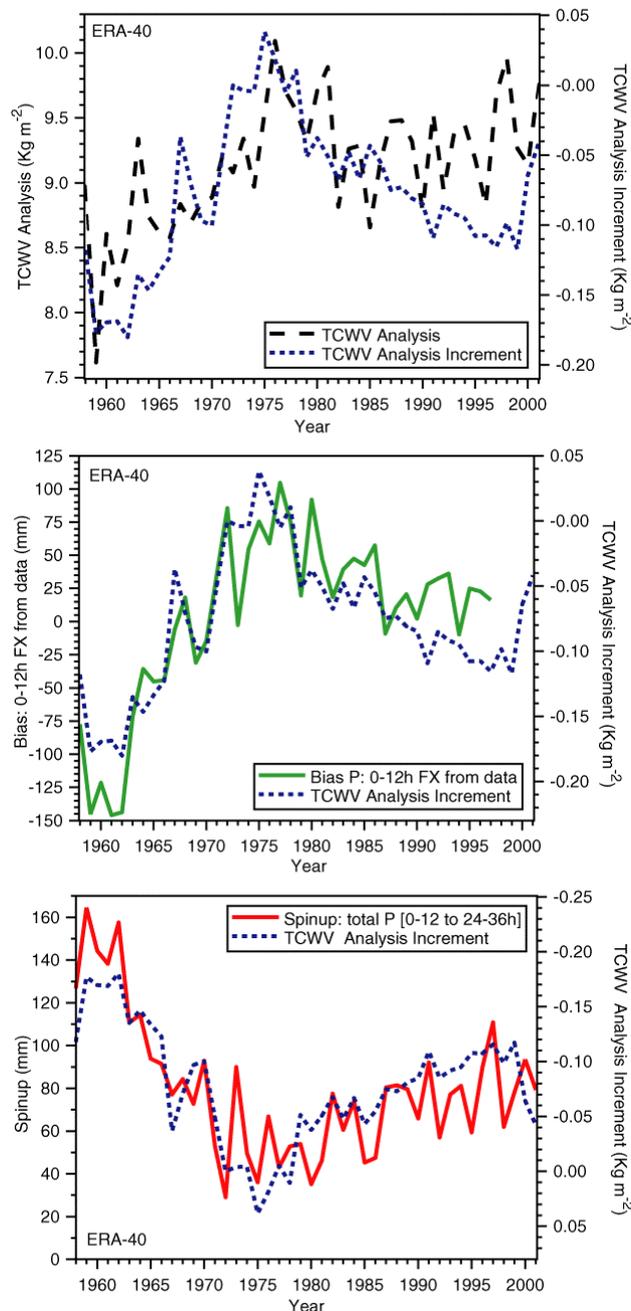

Figure 4 Annual variation of TCWV and its analysis increment (top), model precipitation bias (middle) and model precipitation spinup (bottom).

The annual cycle in TCWV is also seen in the precipitation spinup. Figure 5 (upper panel) shows the monthly variation of spinup and the TCWV analysis increment during the early part of the analysis. The lower panel

shows the correlation between monthly mean spinup and TCWV analysis increment for the whole of ERA-40. Two regression lines are shown, one through the origin.
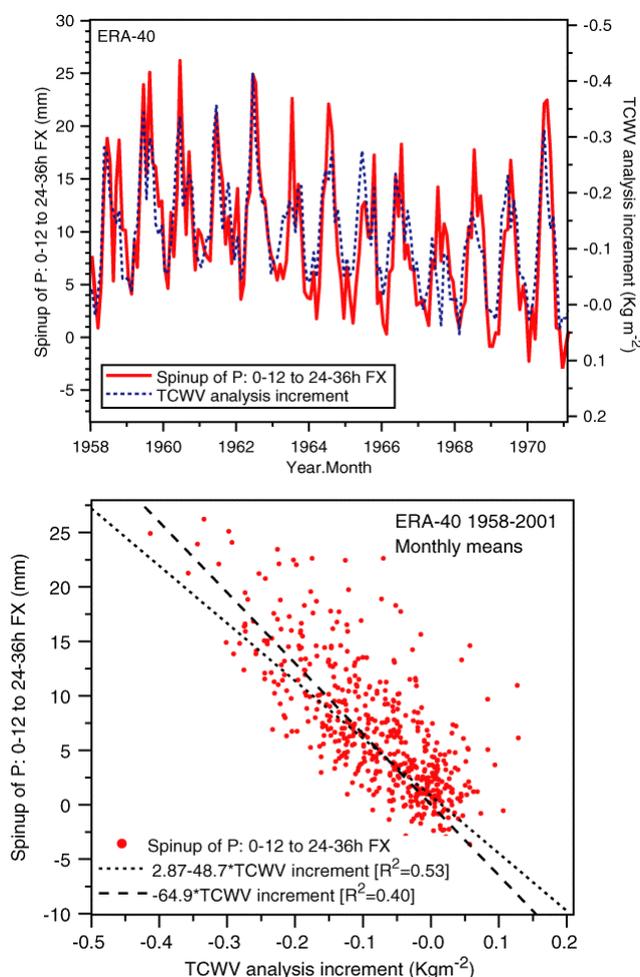

Figure 5 Monthly timeseries of model spinup and TCWV increment (top) and scatterplot of spinup against TCWV increment (bottom).

3.1.2   Annual cycle of precipitation spinup and bias

We will now present data from three periods, 1958-1970; 1974-1981 and 1987-1997, to illustrate differences in the mean annual cycle. Figure 6 shows the mean annual cycle for the three periods of the *observed* Mackenzie precipitation (upper panel), the model precipitation spinup between the 0-12h and 24-36h FX (middle) and the TCWV analysis increment (lower). The Mackenzie precipitation remains low in Spring till May and peaks sharply in July. There is little difference in the mean between the periods. The model spinup shows a marked difference between the periods. Spinup is larger in winter in the 1960s. The first and last periods have a July spinup maximum (as does precipitation), while in the middle period, the spinup is low and has a dip in summer, related to a spindown in convective precipitation (not shown, although it can be seen in the annual average in Figure 3 during this period). The annual cycle of the TCWV incement bears some resemblance to the spinup, but the peak is shifted to June. The reason for this is probably that the model has a distinct seasonal bias in precipitation, shown in Figure 7. The upper panel shows the bias of ERA-40 precipitation in the 0-12h FX. It shows not only the marked difference between the three periods (seen in Figures 3 and 4), but it also shows the bias has a spring peak and a fall minimum. In the 24-36h FX (lower panel), the difference in bias between the

periods has reduced, and it is clear that the model has a high precipitation bias in May-June, and a low bias in August-September. The cause of this is still under investigation.
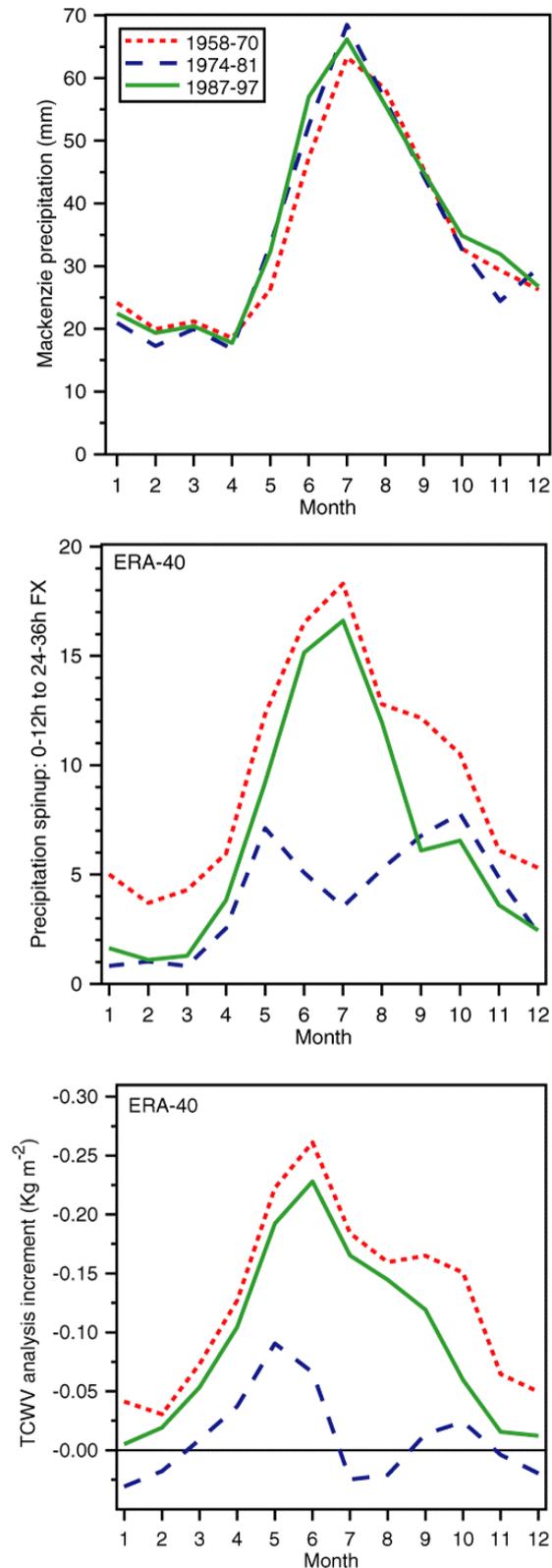

Figure 6 Mean annual cycle of observed Mackenzie precipitation spinup, and TCWV analysis increment for three periods.
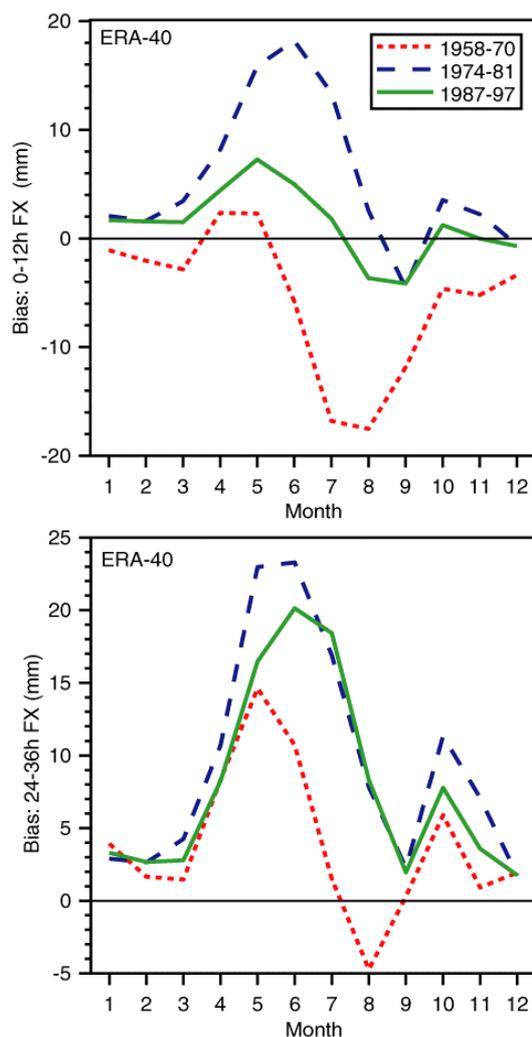
Figure 7 Mean annual cycle of 0-12h FX bias and 24-36h FX bias for three periods.

3.1.3   *Precipitation spinup and bias for three periods*

The left-hand panels of Figure 8 plot monthly precipitation, derived from twice daily 12-24 and 24-36 hour forecasts against the corresponding model precipitation derived from twice-daily 0-12 hour forecasts. Three time periods are shown. Upper left is for the early period, where we see model precipitation increases out to the 24-36 h FX. The slope of the linear regression lines through the origin are shown, together with their R^2 coefficients. Precipitation in the 24-36 h FX is 32% greater than in the 0-12 h FX. The middle left panel for 1974-1981, shows a spinup of only 9%, and this is complete by the 12-24 h FX. The lower left panel shows the more recent period, showing the precipitation spinup increasing from 15 to 19% with forecast time.
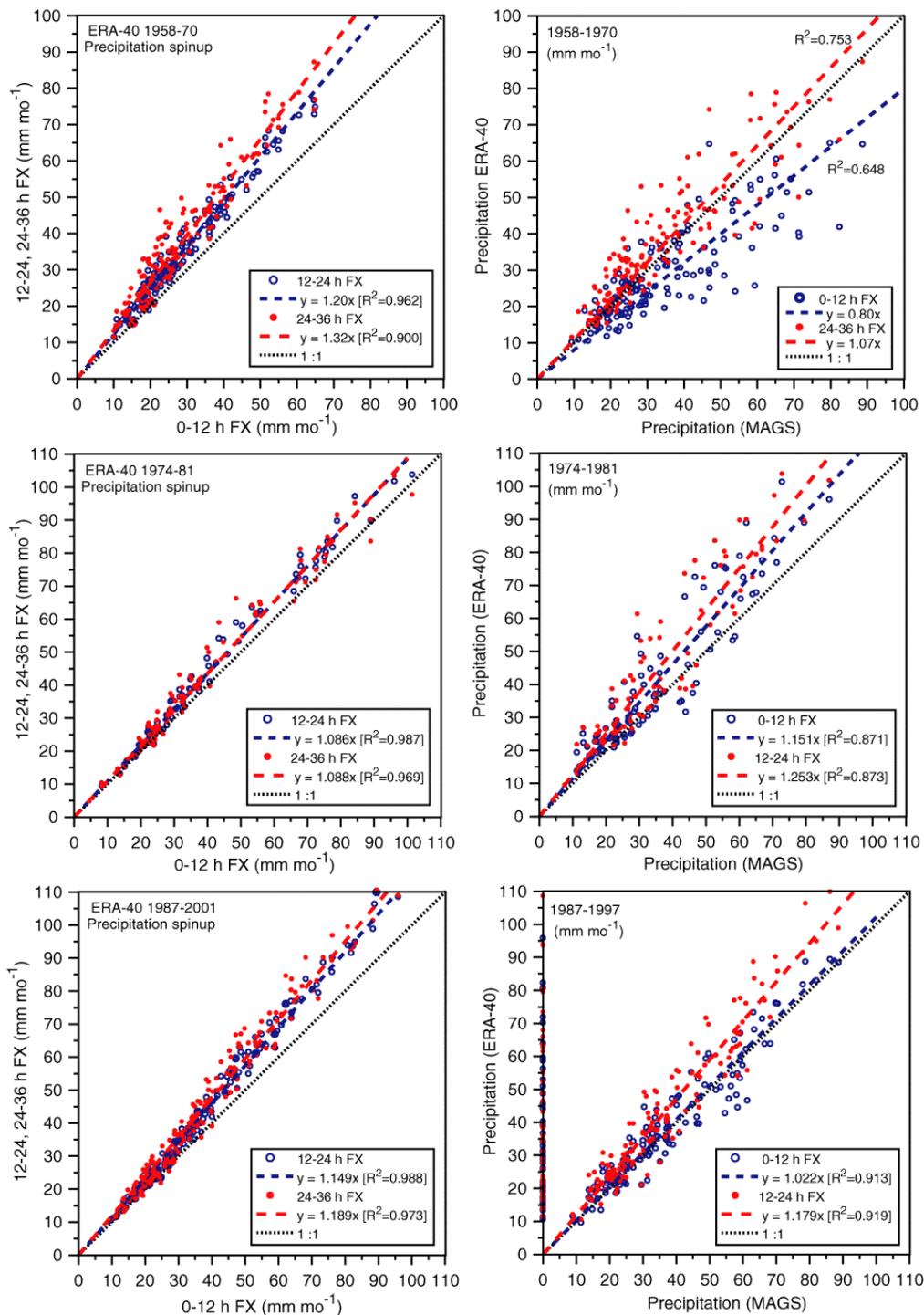
Figure 8 Spinup of ERA-40 precipitation for three epochs (left panels); comparison of ERA-40 with MAGS precipitation estimates (right panels).

3.1.4   Comparison of ERA-40 precipitation and MAGS precipitation

The panels on the right side of Figure 8 plot monthly ERA-40 precipitation against the MAGS basin average observations, together with the linear regression lines. Upper right for the early period shows that the 0-12 h FX precipitation is much lower than the observations, but by the 24-36 h FX becomes comparable, with considerable scatter. For 1974-1981 (middle right), the model precipitation is greater than the observations by 15 % for the 0-

12 h FX and 25% for the 12-24 h FX. The lower right for 1987-1997 (when the MAGS precipitation time-series ends) shows slightly smaller high bias increasing from 2 to 18% with the model spinup. Note that the R^2 correlation coefficient increases systematically with time, reaching 0.91 for the last decade for which we have these monthly averages for the Mackenzie, suggesting that the analysis is improving.

The MAGS precipitation data have been corrected for known errors and biases (Metcalfe et al., 1997; Mekis and Hogg, 1999, Louie et al., 2002). The slopes of the regression lines in the figures are of course dominated by the summer data, when monthly precipitation is highest. We can conclude that the ERA-40 precipitation is best in the last decade in the representation of the month to month variability, when both infrared and microwave satellite radiances are available for the analysis. In terms of bias the issue is less clear, because of the substantial changes in both bias and spinup with time shown in Figures 3 to 7, and the fact that the MAGS precipitation data may not be unbiased despite the correction procedures. The seasonal cycle of the model precipitation bias shown in Figure 7 (high in spring and low in Fall) is however probably real. In the most recent period, the bias of the 0-12h FX precipitation is small, while after spinup, it is likely that ERA-40 has a small high bias for the Mackenzie. We shall look at the individual basins in more detail in section 4.

3.2   Comparison of ERA-40 evaporation with MAGS estimate

Figure 9 shows the annual cycle of the MAGS estimate (Louie et al. 2002) of basin evapotranspiration (ET) for the three periods, and the bias of the ERA-40 0-12h FX total evaporation from the MAGS estimate (lower curves). Standard deviations are shown for the recent period. In winter, the MAGS estimate (itself based on a model, but using station observations), gives a very small downward transport of vapor to the cold surface, while ERA-40 is generally slightly positive with about 5 mm month^{-1} more evaporation than the MAGS estimate. This bias decreases to near zero in spring, before increasing to about 15 mm month^{-1} in summer, with a peak in August-September. Annual evapotranspiration from ERA-40 is higher than a MAGS estimate by 30%. In the summers from 1958-1970, when the ERA-40 precipitation is low, the evaporation bias is also lower. In a later section, we shall conclude from the water balance of the Mackenzie, that the ERA-40 evaporation is probably biased high (see Table 4 later).
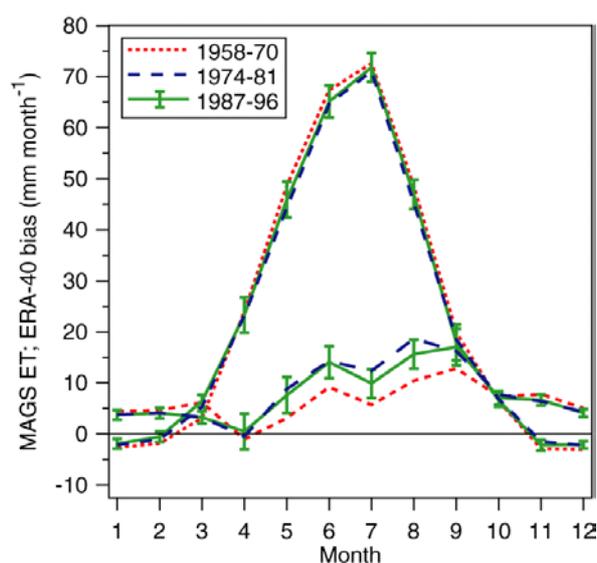

Figure 9 MAGS ET estimate and ERA-40 bias from MAGS estimate

3.3   Comparison of Mackenzie streamflow and ERA-40 runoff

We have streamflow data for the Mackenzie River from 1973 to the present. Figure 10 (upper panel) compares the mean annual cycle (1973-2000) of streamflow for the Mackenzie and the corresponding runoff in ERA-40. The two differ considerably: streamflow at the mouth of the Mackenzie remains very low until May and peaks in June. In contrast, the model runoff, peaks earlier in April (when snow melts in the model), and there is a second smaller peak in August. Louie et al. (2002) suggest that the average drainage time for the basin is of order two months.
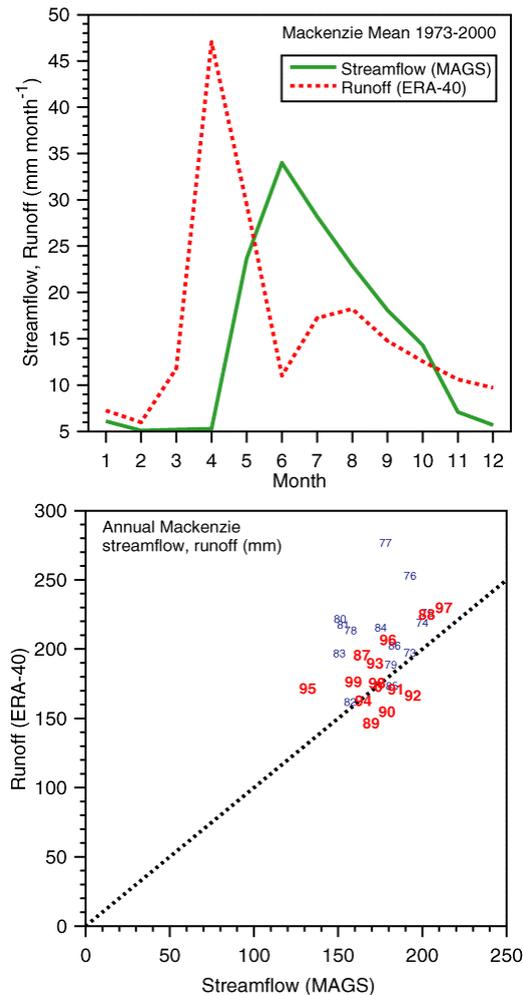

Figure 10 Comparison of Mackenzie streamflow and ERA-40 runoff: annul cycle (top) and annual total (bottom)

The two run-off peaks in ERA-40 are discussed in Van den Hurk et al. (2000). The first model peak occurs when snowmelt runs off 'instantaneously' over the frozen ground. In addition to not having river routing, the model does not represent the freeze-thaw cycles as water penetrates the snowpack and ground and refreezes, which in nature also delay spring runoff. Once the ground thaws, including the deepest soil layer, water can drain through the soil, and above a threshold of liquid water content in the 100-289cm soil layer, deep drainage increases rapidly. This accounts for the second peak in August in the model.

The lower panel compares total annual streamflow on the Mackenzie and model runoff. The numbers correspond to the year, and we have distinguished the period before 1986, when precipitation was higher, from the more recent period from 1987 onward (heavier numerals). Runoff is generally higher in the earlier period, as would be expected from the greater precipitation. In the more recent period, the model runoff and the observed streamflow are comparable, but the interannual variability is not well correlated. One additional complication is that there was an error in the snow analysis initially in ERA-40, which reduced the snow water equivalent of observations introduced in the analysis by a factor of about 0.25. This error was not corrected until the two analysis streams had reached January, 1974 and November, 1994 (Kållberg, 2002, personal communication), so it is likely that snowmelt is reduced for the years 1973 [and partially for 1974] and for 1990-1994. We see that annual runoff is generally lower in these years. Given this error, and the absence of river routing in ERA-40, which plays a major role on the Mackenzie with its large lakes and long residence time before precipitation falling in the south reaches the mouth, we cannot draw many conclusions about this aspect of the hydrological cycle. The annual runoff in ERA-40 is broadly consistent with, but a little higher than, the annual streamflow, and probably snowmelt is too early in the model.

3.4   Surface water reservoirs and analysis increments

In this section, we analyze the surface water reservoirs and their analysis increments. Averages for three periods are shown: 1959-1970, 1974-1981 and 1995-2001.

3.4.1   *Soilwater*

The ERA-40 soilwater analysis modifies soilwater in the first three soil layers (0-7, 7-28 and 28-100 cm), subject to certain constraints, based on analysis increments of 2-m temperature and humidity (Douville et al., 2000).

Figure 11 shows for the three analysis periods the mean annual cycle of column (0-2.89m depth) soilwater (panel a)); and below in panel b), the corresponding soilwater analysis increments. The early period, 1959-70, when precipitation has a large spinup, has the lowest column soilwater, and the largest annual analysis increment (mean of 58mm). In the middle period (1974-81), when precipitation in the analysis cycle is largest compared to observations (Figure 3), soilwater is largest, and the analysis increment is negative in spring and fall and positive in summer with a near-zero annual mean (-1mm). In the recent period, when 0-12 FX precipitation is closest to the MAGS observations, soilwater has intermediate values, and the mean annual increment is 22mm, again with the main contribution in summer. The soil water analysis (Douville et al., 2000), which responds to analysis increments of 2-m temperature and humidity, is playing an important role in the liquid water budget. Soil water is being added in the warmer seasons, and excess soil water is being removed, for example, in the spring in the late 1970's, when precipitation is high. However, since there is evidence that summer evaporation is too high in the model (see Figure 9 and Table 4, later), improvements in the soil water analysis may be possible.
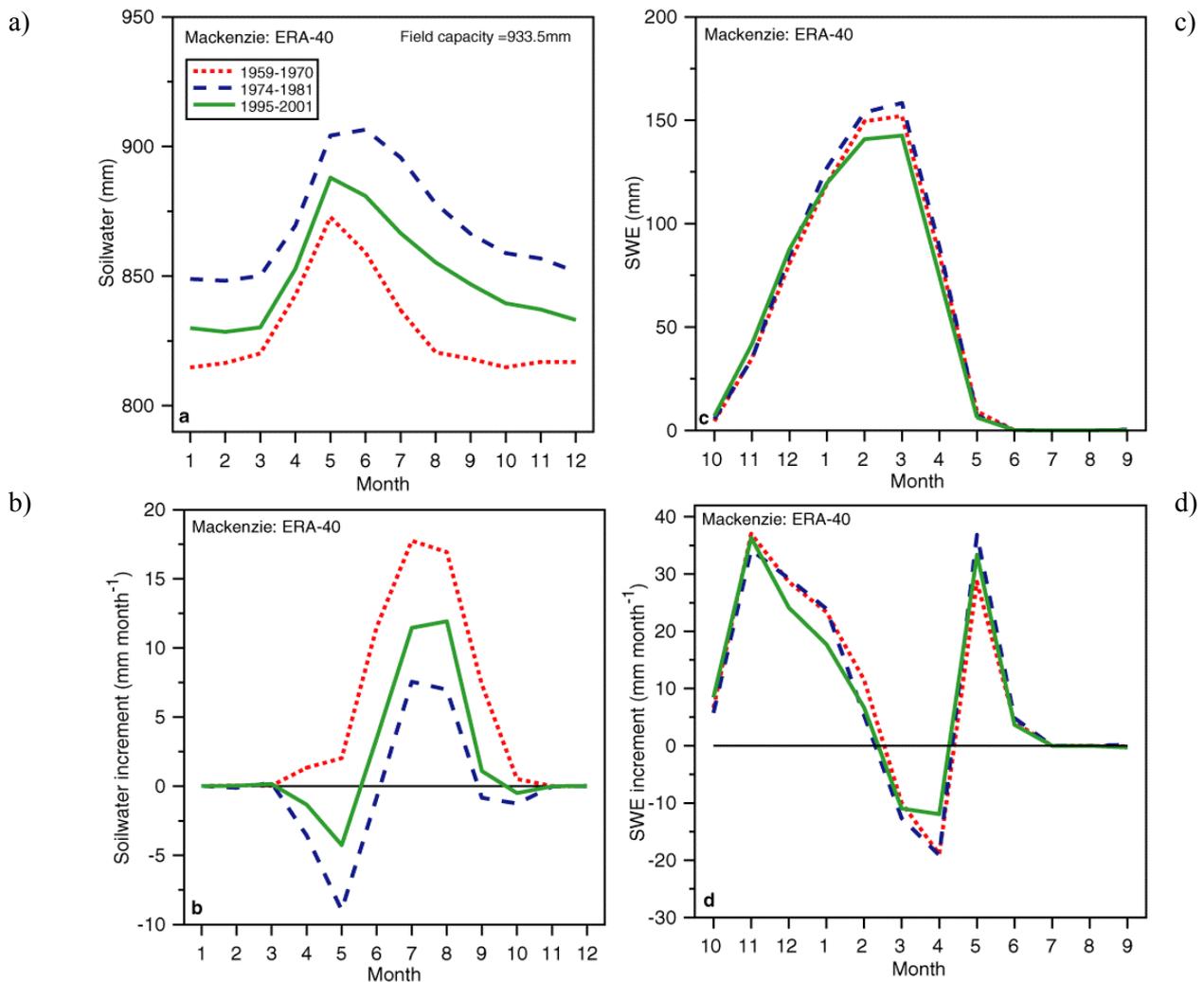
Figure 11 (a) Mean annual cycle of column soilwater, (b) soilwater analysis increment, (c) total snow water equivalent and (d) SWE analysis increment for three data periods.

3.4.2   Snow reservoir

ERA-40 has a single snow layer, with modeled snow water equivalent (SWE) and snow depth, linked by a snow density, which is computed as a function of mean snow age (Van den Hurk et al., 2000). Snow density evolves exponentially from a minimum density for new snow of 100 kg m^{-3} to an aged maximum value of 300 kg m^{-3} with an e-folding time of about 4days, following the formulation of Douville et al. (1995). A snow depth analysis uses snow depth observations, and in addition a nudging towards climatology (with a 12-day timescale), because in many areas the snow observations are inadequate. Snow density is rarely measured, so the analysis uses the model snow density to convert between snow depth and SWE. Figure 11 (right-hand panels (c) and (d)) shows that the annual cycle of SWE in the model and the SWE analysis increments is rather insensitive in the mean to the time period. We have wrapped the time axis to show the year from October to September, to show unbroken the frozen winter period, although the actual data is for calendar years. The interannual variability of SWE is very small for the northern basins, reflecting the fact that the SWE is largely determined by a climatology, but varies considerably for the southern basins where there are snow observations (not shown).

The annual cycle of the SWE analysis increment is peculiar, with the addition of SWE from October to February and May-June, and the removal in March and April. In these averages, the snow analysis adds about 109mm of SWE annually, which is only a little smaller than the mean annual snowfall in the analysis cycle, clearly an undesirable feature. The large addition of SWE in May results from the too-early melt in the model in April (Figure 10). Model snow-depth is too small in May, when compared with the observations, and the analysis adds snow. Although this has an adverse impact on the model hydrology, it reduces the model warm temperature bias (see next section) in May (because there is still observed snow on the surface). The early melt in the model is still under investigation, but it may be related to a simplification in the snow thermal budget. The thermal budget of snow is represented by a single layer (unlike the soil which has four layers, including a shallow first layer of thickness 7cm). To give a reasonable surface diurnal cycle over deep snow and ice, snow depth was also limited to 7cm in the calculation of thermal capacity of the snow layer. While this improves the surface diurnal cycle of temperature, it is likely that it increases the frequency when the snowpack reaches $0^{o}C$ and melts. Snow that melts in the model is removed at once, whereas in nature it might refreeze deeper in the snowpack. Another factor that may be involved in the early snowmelt is that, for many basins, the model has a warm temperature bias in April (see Figures 14 and 18, later).

The winter, early spring positive-negative pattern has probably a more complex origin, relating to the use of model snow density. In winter, except in the earliest epoch, there is no apparent underestimate of model precipitation in the analysis cycle (which might explain a small positive addition of SWE from the snow analysis). However the model compares snow-depth with the observations, and this is critically dependent on the calculation of snow density by the model, which decays with an e-folding time of about 4days to an aged maximum value of 300 kg m^{-3}. If the observed snow does not age as fast as the model assumes (which is likely at the cold temperatures in winter of the Mackenzie basin, see next section), then the observed snow-depths (of low density snow) are effectively interpreted by the analysis (using the higher model snow density) as higher SWE. This would give a spurious positive addition of SWE as long as the density of the observed snow is less than that calculated by the model (which tends to the asymptote of 300 kg m^{-3}). The situation would reverse in March and April as temperatures rise and the observed snow pack ages (shrinking in depth) to a density similar to the model maximum, and the increments become negative to remove the excess snowpack in the model. In fact, it can be shown with a simple model of constant accumulation of snowfall (with no losses), that if the density of the observed snowpack rises in spring to become equal to that calculated by the model, then the winter positive increments and spring negative increments exactly cancel.

3.5   Water budget closure

This section summarizes the closure of the liquid and frozen water budgets in the ERA-40 analysis cycle. We have all components of the water budget for 36 years: 1959-1972, 1974-1988, 1995-2001 (the missing years are those for which the basin averages were not archived for the 6-hour forecasts from the 06 and 18 UTC analyses: see section 2.1).

3.5.1   Liquid and frozen water budget

Figure 12 (upper panel) shows the terms in the 36-year mean annual cycle of the liquid water budget.

$$\Delta CSM = Rain + melt - E_{liquid} - Runoff + SM_{increment} \qquad (1)$$

The mean residual is tiny (not shown), less than about 0.5mm month^{-1}. The rainfall (heavy solid) peaks in summer, while the spring melt peaks in April. In this 36-year mean, these terms are much larger than the soil moisture (SM) analysis increment, which also peaks in summer. Liquid evaporation is a large sink for moisture, again peaking in the summer months. The spring melt contributes to a peak in spring runoff over frozen ground, and to a recharge of the soil moisture reservoir (ΔCSM), which subsequently falls during the summer months.

The lower panel of Figure 12 shows the terms in the corresponding frozen water budget.

$$\Delta\text{SWE} = \text{Snowfall} - E_{\text{frozen}} - \text{Melt} + \text{SWE}_{\text{increment}} \qquad (2)$$

The residual (not shown) is again tiny, peaking at 1mm month^{-1} in April. We have again wrapped the time axis to show the year from October to September. Unlike the liquid budget, the SWE increment is comparable to the snowfall in size, and plays a major role in the budget, as discussed in the previous section. The frozen evaporation is a small term in comparison to the role of the melt in removing the snowpack in spring. This a significant improvement in the frozen budget over an earlier version of the model (Betts and Viterbo, 2000), in which snow evaporation was too large.
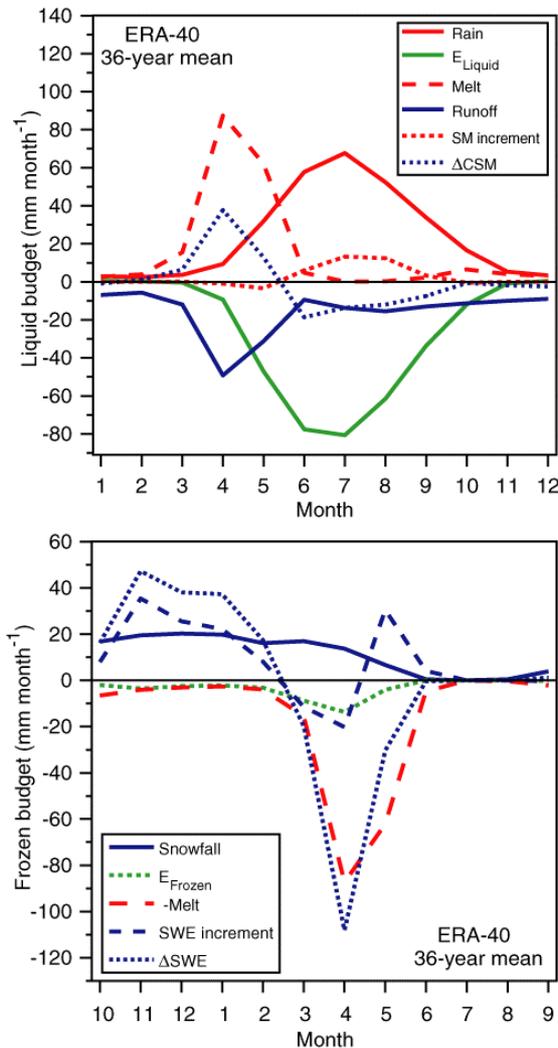

Figure 12 Terms in the liquid (top) and and frozen water budget (bottom).

3.5.2   Comparison with MAGS climatology

Table 4 compares the ERA-40 mean annual water budget for the 24 calendar years, 1971-72, 1974-88, 1995-2001, with the Mackenzie climatology for the 24 water years, October, 1972 to September, 1996, from Louie et al. (2002). We compare the climatologies, because the MAGS budget ends in 1996, and our ERA-40 budget has missing components for 1973 and 1988-1994.

Table 4. Comparison of the ERA-40 water budget with the MAGS water budget climatology.

Mean annual totals (in mm)	ERA-40 Liquid	ERA-40 Frozen	ERA-40 Total	MAGS Climate
Precipitation	323	140	463	422
Evaporation	-327	-38	-366	-274
Melt	194	-194		
Runoff/Streamflow			-207	-176
Analysis increment	17	97	114	
Climate residual				-28
Storage change	0	-2	-2	

We see that the ERA-40 total water budget has 10% more precipitation and 18% more runoff (in this 24-year mean 0-12h FX) than the MAGS 'climate', but 34% more evaporation, and the 'extra' water comes from the analysis increments (mostly from the snow analysis). The MAGS water budget itself has a -28mm residual (-7%), suggesting perhaps that "observed" precipitation is underestimated, because of undercatch. We conclude that it is likely that, while the 0-12h FX ERA-40 precipitation may be realistic, the ERA-40 evaporation has a high bias.

3.6   Temperature comparison

Figure 13 compares the monthly mean 2-m temperature for the Mackenzie basin from ERA-40 and the MAGS observations. All three periods are very similar, so we show only the 1990s. ERA-40 has a realistic interannual variability, but it is slightly cool in summer and warm in winter by 2-3K. The model temperature bias, shown as heavy dashes, has a distinct seasonal pattern, which is similar in all years.
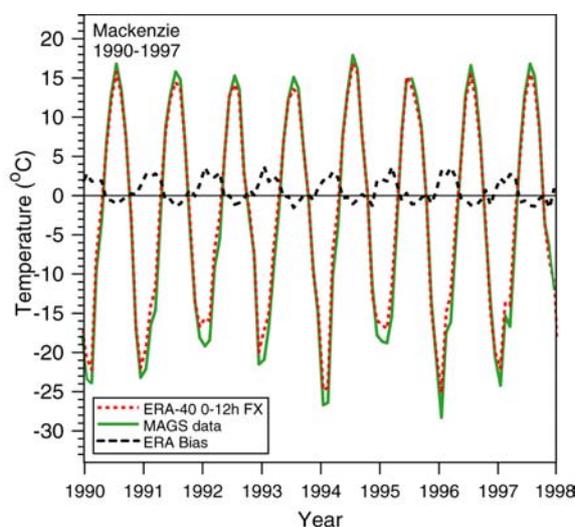

Figure 13 Comparison of temperature for the Mackenzie basin with ERA-40

Figure 14 shows for three periods, the mean annual cycle of the MAGS basin temperature, and the mean bias. The standard deviations are shown for the most recent period, but they do not change significantly with time. The variability in the bias is smaller than the variability in temperature, which is largest in winter. ERA-40 has a distinct warm bias in winter from December to April, peaking in March at +3K. There is a sharp shift in May to a cold bias, which peaks in July at -1.5K. The bias has a curious warm-cold fluctuation from October to November, about 1K in magnitude (this fluctuation occurs in every year, not shown). Clearly changes in the model surface energy balance between warm and cold seasons must be responsible for this distinct annual cycle in the model bias. The cold season warm bias may be due to the model albedo being too low (at about 15% for snow under a forest canopy), an over-correction of the cold bias discussed in Viterbo and Betts, 1999. The summer season cold bias may result from a high bias in evaporation. There is a seasonal phase lag, in that the bias stays cool till November, after the air temperature has fallen well below freezing and there is a snow cover; while the bias stays warm in spring, until the air temperature is above freezing. The transition in December might be related to the ground freezing at depth, as this reduces evaporation which is coupled to liquid water in the soil, but evaporation is already low in November (Figure 9), and the oscillation in October-November suggests that Fall transition is complex. We shall return to this issue when we discuss the individual sub-basins in section 4.3.
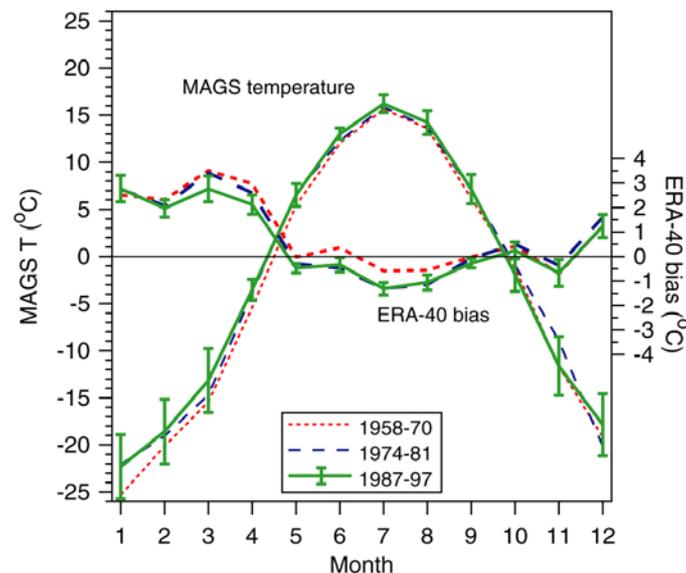

Figure 14 Annual cycle of temperature and ERA-40 bias for three periods

4. Sub-basin comparison of precipitation, evaporation and temperature.

We will now show the variability across the six Mackenzie sub-basins. The Peace River is recombined into one basin (despite the large difference in elevation shown in Table 2), because our MAGS comparison data for the Peace is for the entire river basin.

4.1 Precipitation

Figure 15 plots, for 1990-1997, ERA-40 0-12h FX precipitation for just two of the sub-basins, the Peel basin in the north-west and the Athabasca in the southeast, against the corresponding monthly precipitation from the MAGS observations. Model and observations agree very well for the Athabasca, but precipitation is considerably higher in ERA-40 for the Peel.
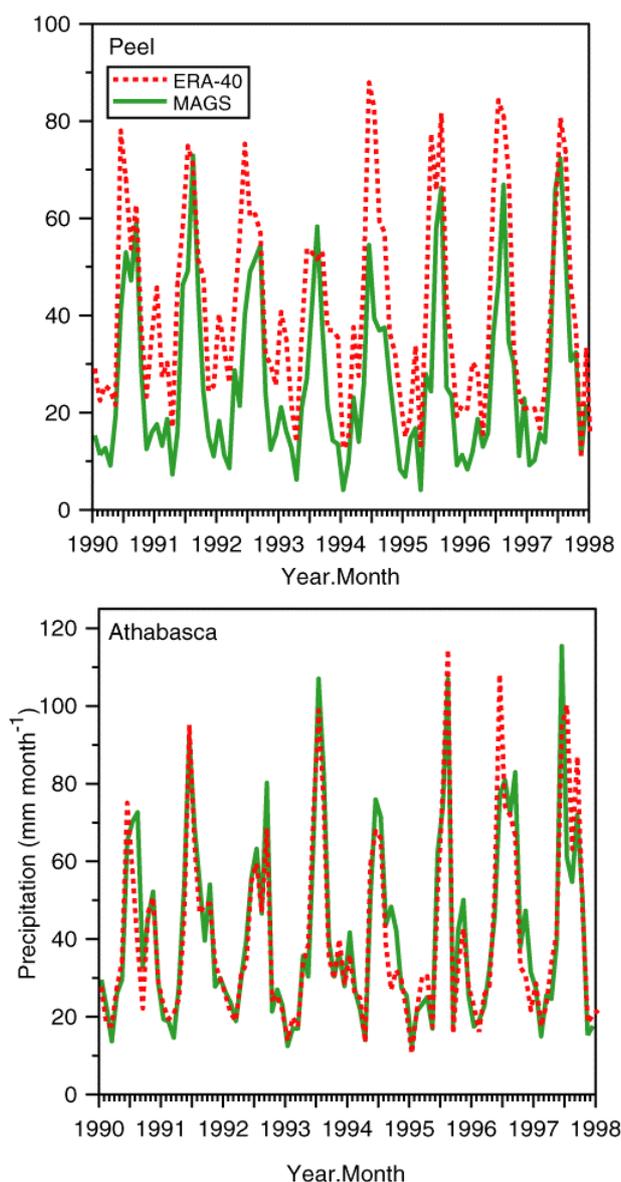
Figure 15 Time series of precipitation for Peel and Athabasca sub-basins from ERA-40 0-12h FX and MAGS data

Figure 16 summarizes the mean annual cycle of precipitation for the six sub-basins for the 28 years, 1970-1997. We have omitted the first 12 years, when there was a large spinup of precipitation. The lower panel is from the MAGS data: the representative standard deviation error bars, shown for the Peel and Peace basins, give an estimate of the interannual variability. The upper panel shows the corresponding mean from ERA-40, and, on the displaced lower right-hand-scale, the bias of ERA-40 from the observations. The bias patterns show that the spring peak and late summer minimum, seen in Figure 7, is a feature of all basins. The spring peak is earlier for the warmer basins (Athabasca and Peace) than the colder basins (Peel and Great Bear Lake). The north-west basins, the Peel, Great Bear Lake and Liard, have generally more precipitation in ERA-40 than the MAGS observations, while the south-eastern basins show primarily the seasonal ERA-40 bias. However, the quality of the MAGS precipitation averages may not be uniform across the sub-basins, because the sparsity of data in the north-west, shown in Figure 2. Precipitation measurement is also challenging in winter (although corrections have been applied for snowfall undercatch), and in mountainous regions. Consequently the differences we see

between ERA-40 and MAGS precipitation estimates for the northern and mountainous basins may stem from problems with (and lack of) data, rather than a bias in ERA-40. The agreement is best for the Athabasca (apart from the seasonal bias in ERA-40), where the data coverage is reasonable.
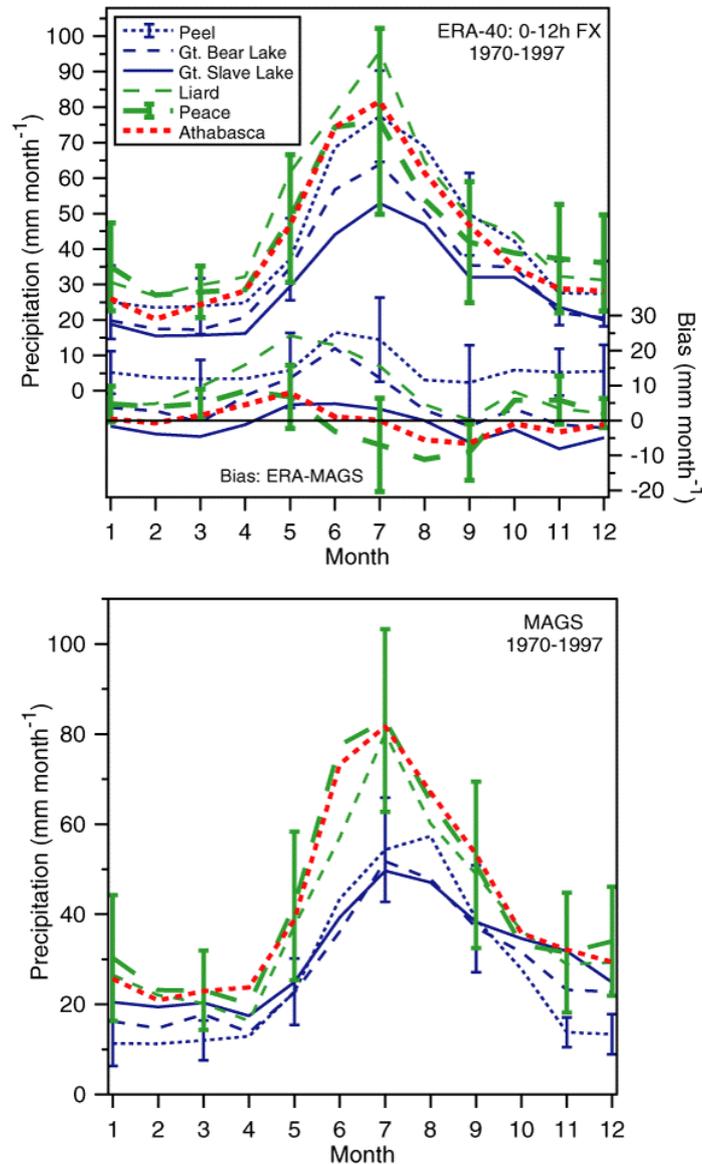

Figure 16 Mean annual cycle of precipitation for Mackenzie sub-basins from MAGS estimate (bottom) and ERA-40 (top), with model bias (right-hand scale).

4.2   Evaporation

Figure 17 compares the ERA-40 total evaporation (upper panel) with the MAGS estimate (lower panel), from Louie et al. (2002) (based on the model of Morton, 1983) for the six sub-basins. In winter, all basins have slightly higher evaporation in ERA-40, while in summer the MAGS estimate shows more variability between basins than ERA-40. We show in the upper panel on the displaced right-hand-scale, the bias of ERA-40 from the MAGS estimate. The bias patterns fall into the same two groups as in Figure 16. In summer, the north-west basins with more precipitation in ERA-40 in Figure 16 have not surprisingly higher evaporation. For the Great Slave, Peace and Athabasca basins, summer evaporation in ERA-40 is similar to the MAGS estimate, but these

basins show a rise in bias in September, which may indicate the lack of a seasonal cycle in the vegetation in ERA-40. The relatively low evaporation in ERA-40 in April (about 20mm month^{-1}), when the soil water is still frozen and unavailable, is an improvement on earlier versions of the model (Betts et al., 1999, 2001a). The standard deviation error bars shown for the Peel and Peace are representative of other basins also.
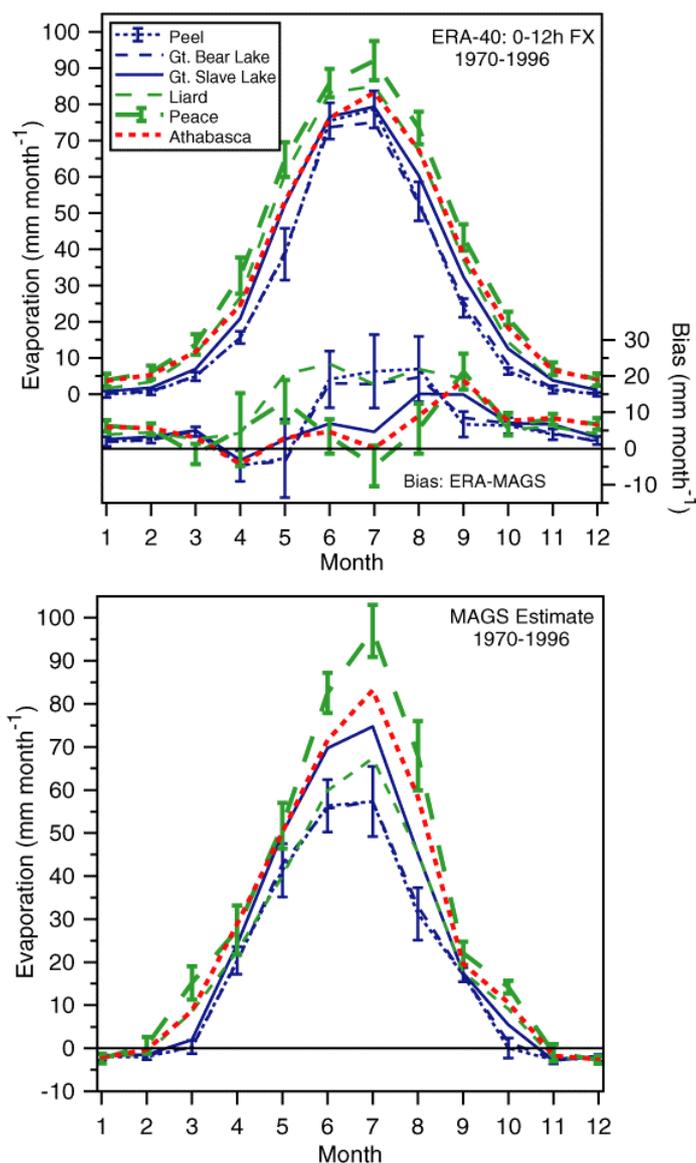

Figure 17 Mean annual cycle of evaporation for Mackenzie sub-basins from MAGS estimate (bottom) and ERA-40 (top), with model bias (right-hand scale).

4.3   Temperature

Figure 18 shows the annual cycle of temperature for the six sub-basins from ERA-40 and the MAGS observations, together with the model bias. The northern basins show little bias, summer and winter, but the southern basins are cool (by -2 to -3K) in summer and relatively warm in winter, especially the Athabasca (bias is +5K). In between, the Liard is cool in summer and the Great Slave basin is warm in winter. So the signal seen in Figure 14 is largely contributed by the more southern basins. The sharp fall in the bias from April to May, and from October to November, also seen in Figure 14, is characteristic of most basins. The standard deviations shown for the Athabasca are representative of other basins. They show that the variability in the model

systematic seasonal bias is smaller than the interannual variability, which is largest in winter. ERA-40 is reproducing most of the interannual variability in temperature, even though the mean biases differ between summer and mid-winter.

At present we have no fully satisfactory explanation for the warmer model bias from December to April compared with the months May to November. By November, the basin is snow covered, and although the ground is still freezing, and evaporation for all basins is already very low (Figure 17). The sun angle is also already low, so the cause of the transition to a warm bias between November and the months December and January (and the October-November oscillation) is unclear. In spring, snow-melt occurs between April and May and the upper layers of the soil melt, with a corresponding large increase in evaporation (Figure 17), so this could be responsible for the shift to a cooler bias in May. There is a large variability between basins. The basins with the warmest bias in winter (Athabasca and Peace) are those with over 90% cover of high vegetation (forests), which have the lowest albedo (0.15 for this vegetation class with snow underneath, Van den Hurk et al., 2000), so it is possible that this winter albedo for the forests is too low.
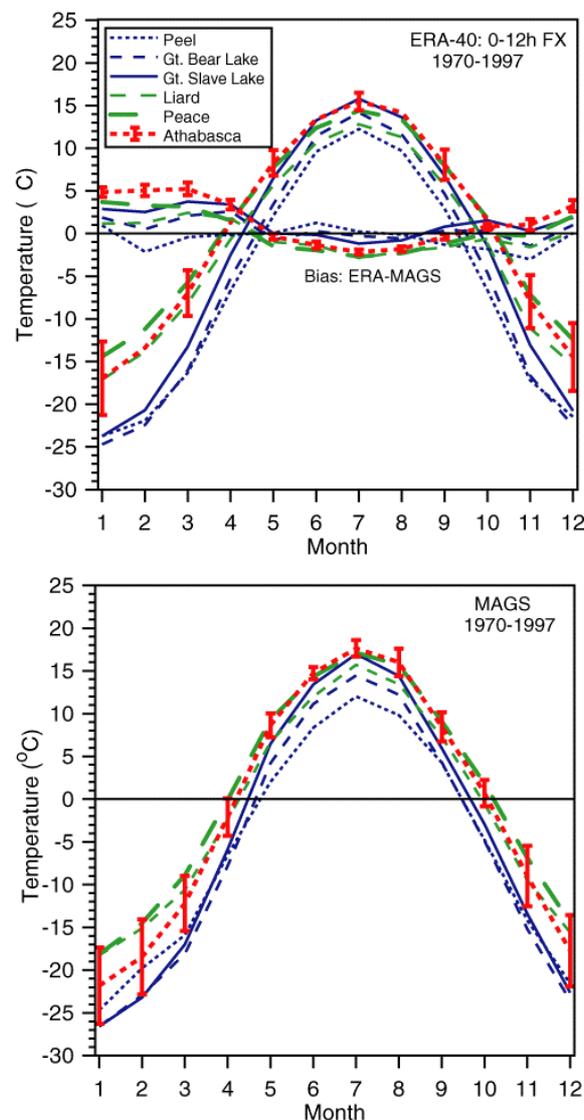

Figure 18 Mean annual cycle of temperature for Mackenzie sub-basins from MAGS estimate (bottom) and ERA-40 (top), showing also model bias.

5. Runoff and streamflow for sub-basins

Streamflow data exists for the Athabasca and Peace Rivers back to 1958 or 1960, and for the other sub-basins to 1973 or 1975 (HYDAT, 2000), so we shall compare streamflow with model runoff for this extended time period. Figures 19 shows the annual comparison, where after 1973, the numerals denote the years. The earliest years (1958-1967), before the assimilation of satellite data, shown as dots for the Peace and Athabasca, have lower model runoff relative to the later years, because precipitation is lower (Figure 3). In general, although a little of the variability in annual streamflow is reproduced in the ERA-40 runoff, most of the basins have a systematic bias (for example, Great Bear and Athabasca are high in ERA-40 and Liard and Peace are low), indicating the simple runoff model handles the variability across the Mackenzie basin poorly. Figure 20 compares the mean annual cycle of observed streamflow and ERA-40 runoff. This comparison has of course many limitations, as runoff is instantaneous in ERA-40, with no river routing, and the major lakes in the sub-basins have a large storage, for which we have no measure. For example, our 'streamflow' for the Great Bear basin is simply a streamflow difference, and its near-zero value in April includes 'negative years', when more water is flowing in from the warmer south, than is flowing out from the colder north. Nonetheless, a few features of ERA-40 can be seen. For most basins, there is a spring peak in April, when snow melts and runs off instantaneously as surface runoff over frozen ground. There is a second peak, coming from deep drainage, later in summer in July or August, when the deep soil layer melts. The water transport and drainage is limited in the case of a partially frozen soil, by considering the effective hydraulic conductivity and diffusivity to be a weighted average of the values for total soil water and a very small value for frozen water. The one exception is the Peace basin, which has no second peak. It is the warmest of the basins in winter (Figure 18), and the deep soil layer freezes only partially in winter (Figure 21, later). For this basin, the spring peak is dominated by deep drainage, with only a small contribution from surface runoff.

In contrast, streamflow is very low in all basins in April and peaks much later in June. Spring melt may be too early in ERA-40, as discussed earlier. In addition, the model does not represent the large accumulation of water that occurs at this time in the snowpack, soil active layer, small ponds and lakes and stream channels (Marsh et al., 2002), which delays drainage by several weeks. For interest, we show (bottom left) the huge change in the annual cycle of streamflow for the Peace River between the first epoch, and the period after 1973. The flow after 1970 is heavily regulated by the completion of the Bennett dam on the western branch of the Peace in the late 1960's.
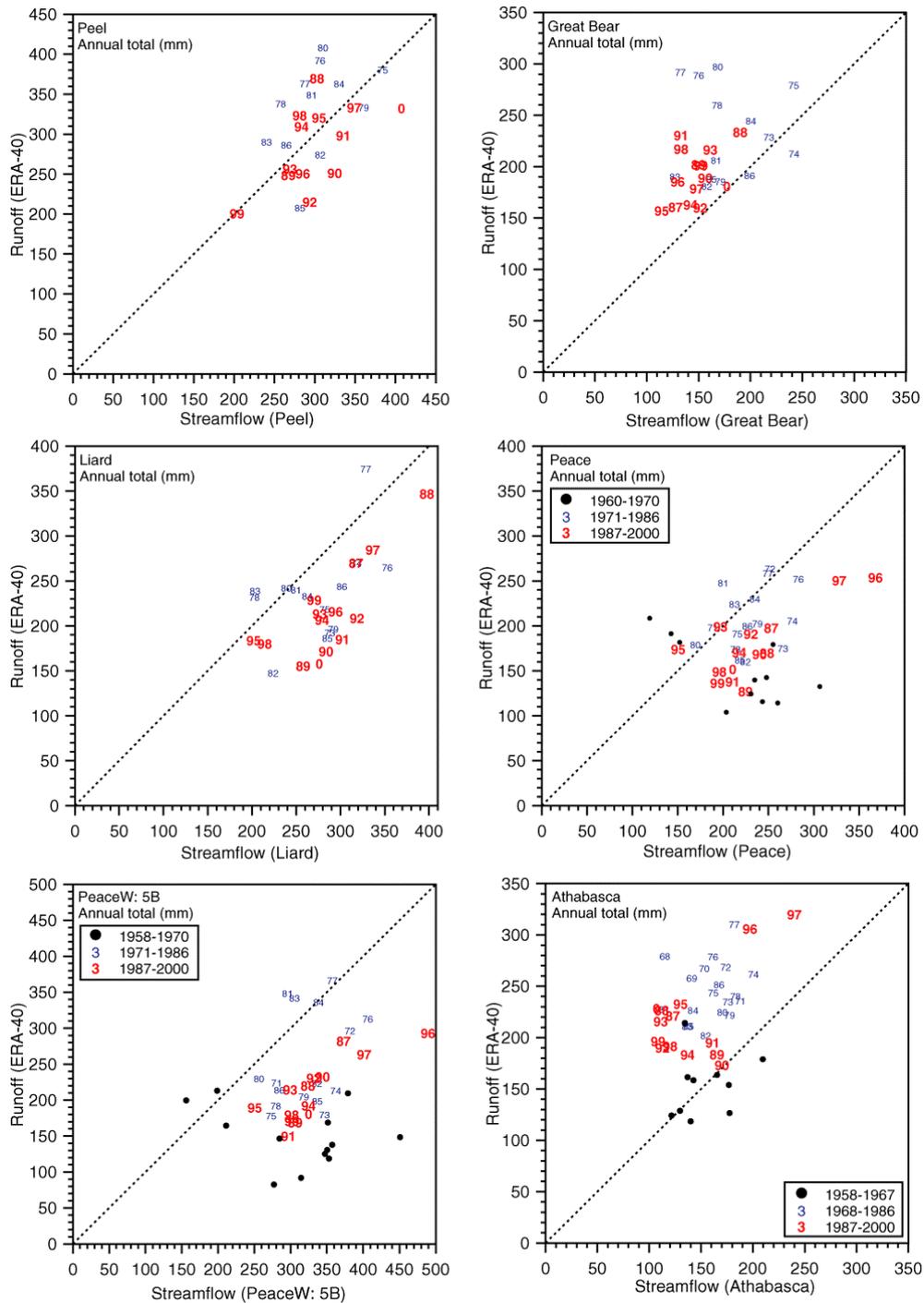
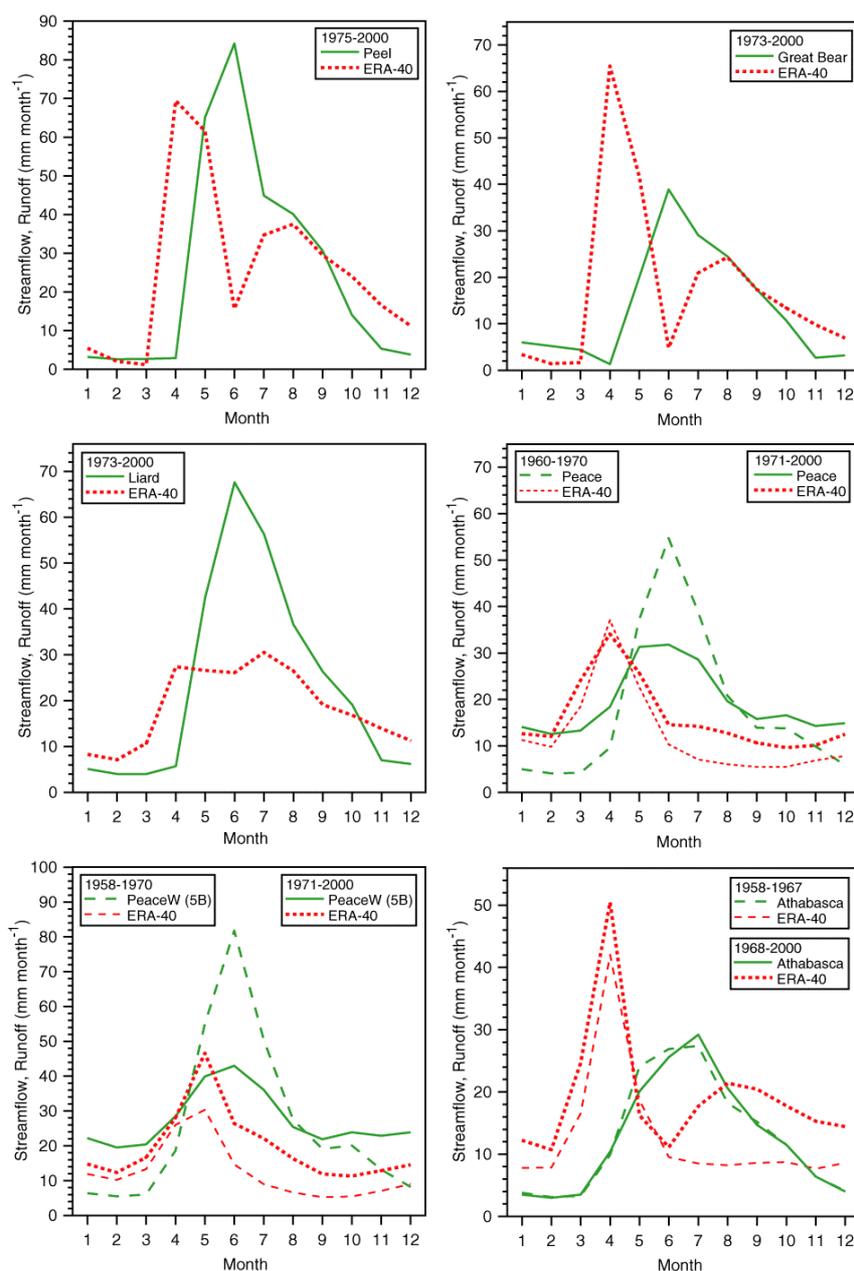Figure 19 Comparison of annual streamflow and ERA-40 runoff.

Figure 20 Comparison of mean annual cycle of streamflow and ERA-40 runoff

6. Soil temperature and Permafrost

The remarkable difference in deep soil temperature (for the 1 to 2.89m layer in the model) across the sub-basins is shown in Figure 21. The northern basins remain largely frozen at depth even in summer, while the western basin of the Peace, the warmest basin, only just freezes at this depth in winter. In between, the Liard has a very small annual cycle of deep soil temperature, because the freeze-thaw cycle introduces a large thermal inertia (Viterbo et al., 1999). This pattern is consistent with the observed climatological gradient across the Mackenzie basin, from continuous permafrost in the north, discontinuous permafrost in the central basin, and no permafrost in the south. Around freezing, ERA-40 uses a diagnostic function to represent the fraction of the soil water that is frozen, with a transition between -3°C and $+1^{\circ}$C (Viterbo et al., 1999).
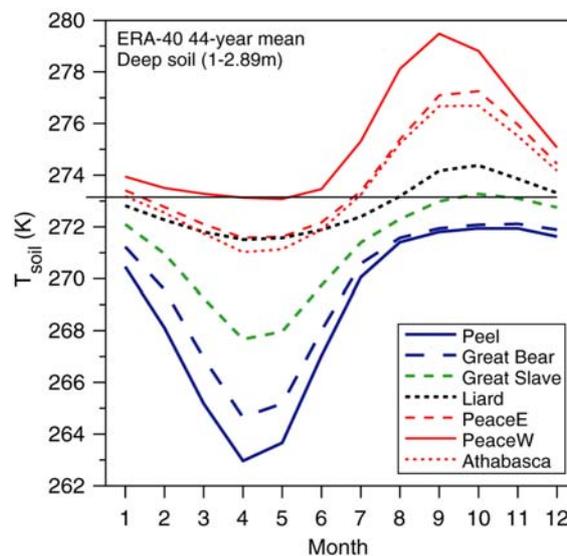
Figure 21 Seasonal cycle of deep soil temperature in ERA-40 for sub-basins.

There is little soil temperature data available for direct comparison in the Mackenzie basin, except in the north, where there is a permafrost monitoring program: CALM (Circum-polar Active Layer Monitoring). Figure 22 compares Peel and Great Bear basin means of ERA-40 deep soil temperature for 1990-1996 with corresponding averages for three CALM sites from Tarnocai (1998) and CAPS (1998). There are some gaps in the data records at the CALM sites, but since the interannual variability at this depth is small, we consider them representative of 1990-1996. The CALM sites are point data at 1.5m depth, and show considerable variation in winter between sites. C-10 and C-12, which are in the Great Bear basin (C-12 at 64° 54' 45" N, 125° 34' 53" W; C-10 at 65° 17' 23" N, 126° 52' 58" W), are warmer than the ERA-40 deepest layer, 1 to 2.89m (both ERA basin means are close); while C-6 (68° 58' 09" N, 133° 32' 54" W), which is just to the north-east of the Peel basin, is much colder. These deep soil temperatures in ERA-40 have a minimum temperature a month later than the CALM sites (but they correspond to a greater depth). In summer, ERA-40 temperatures at this depth are consistent with the CALM data, showing the mean layer temperature remains below freezing.
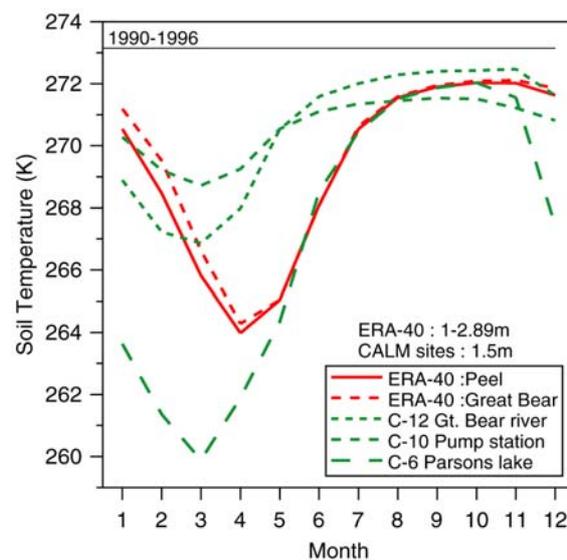

Figure 22 Seasonal cycle of deep soil temperature for the Peel and Great Bear basins compared with point measurements from three CALM sites.

7. Conclusions

We have assessed the systematic biases in temperature and precipitation, and the surface water budget of ERA-40 for the Mackenzie River basin by comparing monthly averages from ERA-40 with basin averages of surface observations of temperature, precipitation, evaporation and streamflow from the Mackenzie GEWEX (Global Energy and Water Cycle Experiment) Study (MAGS). Our first finding was that the bias and spinup of precipitation in ERA-40 changes significantly over the analysis period, because of changes in the assimilated data. On an annual basis, both the bias and spinup of precipitation are correlated with the analysis increment of atmospheric total column water vapor (TCWV). The analysis removes TCWV, which reduces precipitation in the analysis cycle, and the model then spins up to restore precipitation. For the period 1974-1981, when the analysis increment is near zero, the spinup is a minimum. For the same period, the mean bias is +66mm, 16% of the MAGS precipitation, and within the probable error of the observations. ERA-40 has in addition a high bias of precipitation in Spring and a low bias in Fall. The monthly precipitation analysis is best for the most recent decade, when the bias of the 0-12h forecast precipitation is only a few percent higher than the MAGS observations.

We compared evapotranspiration from ERA-40 with a MAGS estimate, from Louie et al. (2002), derived using the semi-empirical model of Morton (1983). ERA-40 has about 5 mm month^{-1} more evaporation than the MAGS estimate in winter, and this bias decreases to near zero in spring, before increasing to about 15 mm month^{-1} in summer, with a peak in the Fall. Annual evapotranspiration from ERA-40 is higher than a MAGS estimate by 30%. From a comparison with the water balance of the Mackenzie as a whole, we conclude that the ERA-40 evaporation is probably biased high.

A detailed comparison of the ERA-40 runoff with the Mackenzie streamflow is not possible, as the model has no river routing, and there is a long residence time for water in the Mackenzie (with its large lakes) before precipitation falling in the south reaches the mouth. The annual runoff in ERA-40 is comparable to the annual streamflow, but the interannual variability is poorly correlated. ERA-40 has two runoff peaks: in April, when snowmelt runs off quickly over the frozen ground, and in August, when the lowest model layer melts and reaches a soil moisture threshold, when deep drainage increases rapidly.

In model liquid water budget (a mean for 24 years), the soil water analysis increment contributes only 17mm of water to the annual liquid budget (primarily in summer), small compared with the mean rainfall (323mm) and snowmelt (194mm). However in the frozen budget, the analysis increment of snow water equivalent, with an annual mean total of 97mm, is not much smaller than the mean annual snowfall (140mm). This is clearly an undesirable feature, which impacts the liquid budget through the snowmelt. Improvements to the model snow treatment are needed: snow melts too soon in the model, and is replaced by the snow analysis increments. The thermal properties of the snow are not well represented by a single layer. A better snow density model is also needed, since this is also used to analyze snow-depth observations. It is likely that the aging of the density of the model snowpack (with a 4-day timescale) is too fast at the cold temperatures of the Mackenzie basin. For the northern basins, there are insufficient snow depth observations, so the analysis depends on climatology.

For the Mackenzie, ERA-40 has a distinct seasonal temperature bias, with a 2 to 3K warm bias from December to April, and a cool bias in summer, reaching -1.5K in July. This signal is most pronounced for the heavily forested southern basins. Although this is presumably related to the different model parameterizations for the winter forest with snow under tall vegetation, and to the freezing and thawing of the ground, we do not yet fully understand

the details. The warm winter bias may be related to a too-low albedo for snow under tall vegetation, which was greatly reduced to correct a much larger cold bias in an earlier version of the land-surface model (Viterbo and Betts, 1999). The cool summer bias may reflect excess evaporation. In a comparison of the sub-basins with the MAGS estimates, ERA-40 has more precipitation than the MAGS observations for the northern and western mountainous basins, but for those basins the data are sparse. For evaporation, ERA-40 has less variation across the basins than the MAGS estimate.

Several aspects of the ERA-40 hydrology are sensitive to soil temperatures: surface runoff occurs only over frozen ground, while deep runoff depends on the lowest layer melting, and transpiration depend on liquid water in the root zone. ERA-40 appears to represent well the climatological gradient of deep soil temperature across the Mackenzie basin, from continuous permafrost in the north, discontinuous permafrost in the central basin, and no permafrost in the south.

The boreal forest and the Arctic is a challenging environment for model physical parameterization. Substantial efforts at ECMWF to improve the surface model in cold regions (e.g., Viterbo and Betts, 1999; Viterbo et al. 1999, Van den Hurk et al. 2000) have paid off in ERA-40 improvements relatively to ERA-15, such has a reduction of the temperature errors in winter, and the evaporation overestimation in spring. Nevertheless, deficiencies remain and their correction are the focus of future research in the areas of snow parameterization (improved treatment of melting and snow density) and data assimilation (usage of snow cover based on remote sensing; Robinson et al., 1993).

Acknowledgments

References

Betts, A. K. and P. Viterbo, 2000: Hydrological budgets and surface energy balance of seven subbasins of the Mackenzie River from the ECMWF model. *J. Hydrometeorol*., **1**, 47-60.

Betts A. K., P. Viterbo, A.C.M. Beljaars, H-L. Pan, S-Y. Hong, M. L.Goulden and S.C. Wofsy, 1998: Evaluation of the land-surface interaction in the ECMWF and NCEP/NCAR reanalyses over grassland (FIFE) and boreal forest (BOREAS). *J. Geophys. Res*., **103**, 23079-23085.

Betts, A. K., M. L. Goulden, and S.C. Wofsy, 1999: Controls on evaporation in a boreal spruce forest. *J. Climate*, **12**, 1601-1618.

Betts, A. K., J. H. Ball, and J. H. McCaughey, 2001a: Near-surface climate in the boreal forest. *J. Geophys. Res.*, **106**, 33529-33542.

Betts , A. K., P. Viterbo, A.C.M. Beljaars and B.J.J.M. Van den Hurk, 2001b: Impact of BOREAS on the ECMWF Forecast Model. *J. Geophys. Res.*, **106,** 33593-33604.

Betts, A. K., J. H. Ball, M, Bosilovich, P. Viterbo, Y. Zhang, and W. B. Rossow, 2003: Intercomparison of Water and Energy Budgets for five Mississippi Sub-basins between ECMWF Reanalysis (ERA-40) and NASA-DAO fvGCM for 1990-1999. *J. Geophys. Res.*, **108**, xxxx, doi:10.1029/2002JD003127 (in press).

Cao, Z., M. Wang, B. A. Proctor, G. S. Strong, R. E. Stewart, H. Ritchie and J. E. Burford, 2002. On the Physical Processes Associated with the Water Budget and Discharge of the Mackenzie Basin during the 1994/95 Water Year. *Atmosphere-Ocean*, **40**, 125-143.

CAPS, 1998. *Circumpolar active-layer permafrost system (CAPS), version 1.0*. International Permafrost Association, Data and Information Working Group, comp. 1998. Boulder, CO: National Snow and Ice Data Center/World Data Center for Glaciology. CD ROM.

Douville, H. J.-F. Royer and J.-F. Mahfouf, 1995: A new snow parameterization for the Meteo-France climate model. Part I: validation in stand-alone experiments; *Clim. Dynamics*, **12**, 21-35.

Douville, H., P. Viterbo, J.-F. Mahfouf, and A.C.M. Beljaars, 2000: Evaluation of optimal interpolation and nudging techniques for soil moisture analysis using FIFE data. *Mon. Wea. Rev.*, **128**, 1733-1756 .

HYDAT, 2000, Canadian Streamflow CD-ROM, available from Climate and Water Products Division, Environment Canada, 4905 Dufferin Street, Downsview, Ontario M3H 5T4.

Louie, P.Y.T., B.E. Goodison, J.R. Metcalfe and S. Ishida, 1996, Corrected precipitation for the Canadian Mackenzie basin GEWEX Study area. In: *Proc. of the Second International Conference on the Global Energy and Water Cycle*, 17-21 June 1996, Washington, DC, USA, pp.234.

Louie, P.Y.T., W.D. Hogg, M.D. MacKay, X. Zhang and R. Hopkinson, 2002: The water balance climatology of the Mackenzie basin with reference to the 1994/95 Water Year. *Atmosphere-Ocean*, **40**, 159-180.

Marsh, P., C. Onclin and N. Neumann, 2002, Water and Energy Fluxes in the Lower Mackenzie Valley, 1994/95. *Atmosphere-Ocean*, **40**, 245-256.

Metcalfe, J.R., B. Routledge and K. Levine, 1997: Rainfall measurement in Canada: changing observational methods and archive adjustment procedures. *J. Climate,* **10**, 92-101.

Mekis, E. and W.D. Hogg, 1999. Rehabilitation and analysis of Canadian daily precipitation time series. *Atmosphere-Ocean*, **37**, 53-85.

Morton, F.I., , 1983: Operational estimates of areal evapotranspiration and their significance to the science and practice of hydrology. *Journal of Hydrology*, **66**, p 1-76.

Robinson, D.A., K.F. Dewey, and R.R. Heim, Jr., 1993: Global snow cover monitoring: an update. *Bull. Amer. Meteorol. Soc.*, **74**, 1689-1696.

Rouse, W.R., 2000a: Progress in hydrological research in the Mackenzie GEWEX Study. *Hydrological Processes*, **14**, 1667-1685.

Rouse, W.R., 2000b. The energy and water balance of high latitude wetlands: controls and extrapolation. *Global Change Biology*, **6** (Supp. 1), 174-184.

Rouse, W.R., E.M. Blyth, R.W. Crawford, J. R. Gyakum, J.R. Janowicz, B. Kochtubajda, H.G. Leighton, P. Marsh, L. Martz, A. Pietroniro, H. Ritchie, W.M. Schertzer, E.D. Soulis, R.E. Stewart, G.S. Strong, and M.K. Woo, 2003: Energy and Water Cycles in a High Latitude, North-Flowing River System: Summary of Results from the Mackenzie GEWEX Study - Phase 1. *Bull. Amer. Meteorol. Soc.*, 2003, **84**, 73-87.

Simmons A.J. and J.K. Gibson, 2000: The ERA-40 Project Plan, ERA-40 Project Report Series No. 1, ECMWF, Reading RG2 9AX, UK., 63pp.

Seglenieks, F. and E.D. Soulis, 2000: Generation of square grid normals for Canada - Phase 1. Contractor's report to Meteorological Services of Canada, 102pp.

Stewart, R.E., 2002: Towards Understanding Water and Energy Processes within the Mackenzie River Basin. *Atmosphere-Ocean*, **40**, 91-94.

Stewart, R.E., H.G. Leighton, P. Marsh, G.W.K. Moore, H. Ritchie, W.R. Rouse, E.D. Soulis, G.S. Strong, R.W. Crawford, and B. Kochtubajda, 1998: The Mackenzie GEWEX Study: the water and energy cycles of a major North American river basin. *Bull. Amer. Meteor. Soc.,* **79**, 2665-2684.

Stewart, R.E., J.E. Burford, and R.W. Crawford, 2000: On the characteristics of the water cycle of the Mackenzie River Basin. *Meteorol. Z.*, **9**, 103-110.

Strong, G.S., B. Proctor, M. Wang, E.D. Soulis, C.D. Smith, F. Seglenieks, and K. Snelgrove, 2002: Closing the Mackenzie basin water budget, Water Years 1994-95 through 1996-97. *Atmosphere-Ocean*, **40**, 159-180.

Tarnocai, C., 1998: Active layer monitoring, Mackenzie Valley, Canada. Boulder, CO: National Snow and Ice Data Center/World Data Center for Glaciology. Digital Media.

Van den Hurk, B.J.J.M., P. Viterbo, A.C.M. Beljaars and A. K. Betts, 2000: Offline validation of the ERA40 surface scheme. *ECMWF Tech Memo, 295*, 43 pp., Eur. Cent. For Medium-Range Weather Forecasts, Shinfield Park, Reading RG2 9AX, England, UK.

Viterbo, P. and A.K. Betts, 1999: The impact on ECMWF forecasts of changes to the albedo of the boreal forests in the presence of snow. *J. Geophys. Res.*, **104**, 27 803-27 810.

Viterbo, P., A.C.M. Beljaars, J-F Mahfouf, and J. Teixeira, 1999: The representation of soil moisture freezing and its impact on the stable boundary layer. *Quart. J. Roy. Meteor. Soc.*, **125**, 2401-2426.

Walsh, J. E., V. Kattsov, D. Portis, and V. Meleshko, 1998: Arctic precipitation and evaporation: model results and observational estimates. *J. Climate*, **11**, 72-87.